

**AEDC-TR-93-19**

**AD-A274 591**



2



# **An Algorithm for Determination of Bearing Health Through Automated Vibration Monitoring**

**S. W. Hite, III**  
**Sverdrup Technology/AEDC Group**

**December 1993**

**Final Report for Period October 1, 1992 – September 30, 1993**

**DTIC**  
**ELECTE**  
**JAN 10 1994**  
**S E D**

Approved for public release; distribution is unlimited.

**94-00881**



67px

**ARNOLD ENGINEERING DEVELOPMENT CENTER**  
**ARNOLD AIR FORCE BASE, TENNESSEE**  
**AIR FORCE MATERIEL COMMAND**  
**UNITED STATES AIR FORCE**

**94 1 7 33 2**

## NOTICES

When U. S. Government drawings, specifications, or other data are used for any purpose other than a definitely related Government procurement operation, the Government thereby incurs no responsibility nor any obligation whatsoever, and the fact that the Government may have formulated, furnished, or in any way supplied the said drawings, specifications, or other data, is not to be regarded by implication or otherwise, or in any manner licensing the holder or any other person or corporation, or conveying any rights or permission to manufacture, use, or sell any patented invention that may in any way be related thereto.


Qualified users may obtain copies of this report from the Defense Technical Information Center.

References to named commercial products in this report are not to be considered in any sense as an endorsement of the product by the United States Air Force or the Government.

This report has been reviewed by the Office of Public Affairs (PA) and is releasable to the National Technical Information Service (NTIS). At NTIS, it will be available to the general public, including foreign nations.

## APPROVAL STATEMENT

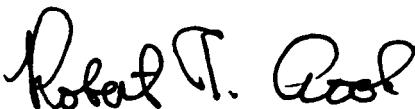
This report has been reviewed and approved.



JAMES D. MITCHELL  
Propulsion Flight  
Technology Division  
Test Operations Directorate

Approved for publication:

FOR THE COMMANDER



ROBERT T. CROOK  
Chief, Technical Management Flight  
Technology Division  
Test Operations Directorate

REPORT DOCUMENTATION PAGE			Form Approved OMB No. 0704-0188	
Public reporting burden for this collection of information is estimated to average 1 hour per response, including the time for reviewing instructions, searching existing data sources, gathering and maintaining the data needed, and completing and reviewing the collection of information. Send comments regarding this burden estimate or any other aspect of this collection of information, including suggestions for reducing this burden, to Washington Headquarters Services, Directorate for Information Operations and Reports, 1215 Jefferson Davis Highway, Suite 1204, Arlington, VA 22202-4302, and to the Office of Management and Budget, Paperwork Reduction Project (0704-0188), Washington, DC 20503.				
1. AGENCY USE ONLY (Leave blank)		2. REPORT DATE December 1993		3. REPORT TYPE AND DATES COVERED Final Report - Oct. 1, 1992 - Sept. 30, 1993
4. TITLE AND SUBTITLE  An Algorithm for Determination of Bearing Health Through Automated Vibration Monitoring			5. FUNDING NUMBERS  65807F 0088	
6. AUTHOR(S)  Sid W. Hite, III Sverdrup Technology, Inc., AEDC Group				
7. PERFORMING ORGANIZATION NAME(S) AND ADDRESS(ES)			8. PERFORMING ORGANIZATION (REPORT NUMBER)  AEDC-TR-93-19	
9. SPONSORING/MONITORING AGENCY NAMES(S) AND ADDRESS(ES)  Arnold Engineering Development Center/DOT Air Force Materiel Command Arnold Air Force, TN 37389-9011			10. SPONSORING/MONITORING AGENCY REPORT NUMBER	
11. SUPPLEMENTARY NOTES  Available in Defense Technical Information Center (DTIC).				
12a. DISTRIBUTION/AVAILABILITY STATEMENT  Approved for public release; distribution is unlimited.			12b. DISTRIBUTION CODE	
13. ABSTRACT (Maximum 200 words)  This report investigates considerations involved in designing an expert system capable of real-time monitoring of turbine engine vibration data to detect rolling element bearing faults. Topics include development of the fundamental bearing fault frequencies, data analysis techniques, results of manual analysis, and considerations in bearing health criteria and monitoring. Methodologies are described for characterization of engine family vibration across the engine's envelope, and a bearing health monitoring algorithm is discussed in detail.  Work reported will be extended and automated to encompass a complete vibration-based turbine engine <u>Health Monitoring System</u> (HEMOS). When completely developed, HEMOS will likely augment the multifaceted capabilities of the Computer Assisted Dynamic Data Monitoring and Analysis System (CADDMAS) under development by the Directorate of Technology - Propulsion Division (DOTP) of Arnold Engineering Development Center (AEDC), Air Force Materiel Command (AFMC), Arnold AFB, TN.				
14. SUBJECT TERMS  acceleration, amplitude, bearing displacement, expert system, vibration, fault frequency, and velocity			15. NUMBER OF PAGES 70	
			16. PRICE CODE	
17. SECURITY CLASSIFICATION OF REPORT UNCLASSIFIED	18. SECURITY CLASSIFICATION OF THIS PAGE UNCLASSIFIED	19. SECURITY CLASSIFICATION OF ABSTRACT UNCLASSIFIED	20. LIMITATION OF ABSTRACT SAME AS REPORT	

## PREFACE

The work reported herein was conducted at the Arnold Engineering Development Center (AEDC), Air Force Materiel Command (AFMC), under Program Element 65807F, at the request of AEDC/DOT, Arnold Air Force Base, TN. The AEDC/DOT Project Manager was J. D. Mitchell. Management for this project was performed by Sverdrup Technology, Inc., AEDC Group, support contractor of the propulsion test facilities, AEDC, AFMC, Arnold Air Force Base, TN, under Air Force Project No. 0088. The Sverdrup Project Manager was T. F. Tibbals. The manuscript was submitted for publication on October 25, 1993.

DTIC QUALITY INSPECTED 5

Accession For	
NTIS   CRA&I	<input checked="" type="checkbox"/>
DTIC   TAB	<input checked="" type="checkbox"/>
Unannounced	<input type="checkbox"/>
Justification _____	
By _____	
Distribution /	
Availability Codes	
Dist	Avail and / or Special
<b>A-1</b>	

## CONTENTS

	<u>Page</u>
<b>PREFACE</b> .....	1
<b>1.0 INTRODUCTION</b> .....	7
1.1 Historical Background .....	7
1.2 Statement of Problem .....	8
1.3 Engine Overview .....	9
1.4 Limitations of the Research .....	9
1.5 Approach .....	10
<b>2.0 ROLLING ELEMENT BEARING FAULT FREQUENCIES</b> .....	11
2.1 General—Bearing Geometry and Motion .....	12
2.2 Cage Speed .....	12
2.3 Rolling Element Speed .....	14
2.4 Special Application .....	15
2.5 Fundamental Train Frequency (FTF) .....	16
2.6 Ball Pass Frequency—Outer Race (BPFO) .....	16
2.7 Ball Pass Frequency—Inner Race (BPFI) .....	16
2.8 Ball Spin Frequency (BSF) .....	17
2.9 Bearing Fault Diagnosis .....	17
<b>3.0 DATA ANALYSIS TECHNIQUES</b> .....	18
3.1 Physical Quantities of Vibration .....	18
3.2 Data Presentation Alternatives .....	21
3.3 Primary Bearing Vibratory Responses .....	21
3.4 Methodologies for Limit Application .....	23
3.5 Modes of Algorithm Operation .....	24
<b>4.0 ANALYTICAL RESULTS</b> .....	26
4.1 Background .....	26
4.2 Operating Parameter Effects on Vibrations .....	26
4.3 Response Amplitude Repeatability .....	28
4.4 Necessity for Automation .....	28
<b>5.0 BEARING HEALTH CRITERIA AND MONITORING</b> .....	29
5.1 Baseline Vibration Considerations .....	29
5.2 Bearing Health Characterization Algorithm .....	29
5.3 Role of Operating Environment .....	32
5.4 Fault Frequency Combinations .....	32
5.5 Real-Time Bearing Health Monitoring Algorithm .....	33
5.6 Other Considerations .....	35
5.7 CADDMAS—A Vehicle for HEMOS .....	36

	<u>Page</u>
<b>6.0 SUMMARY AND CONCLUSIONS</b> .....	<b>37</b>
6.1 Summary .....	37
6.2 Conclusions .....	38
REFERENCES .....	40

## ILLUSTRATIONS

<u>Figure</u>	<u>Page</u>
1. Phases of Machine Deterioration .....	43
2. Failed Ball Element Thrust Bearing .....	44
3. Simplified Schematic of a Turbofan Engine .....	45
4. Rolling Element Bearing Geometry and Motion .....	46
5. Typical "Healthy" Bearing Spectrum .....	47
6. Deteriorated Bearing Spectrum .....	47
7. Vibration Unit Conversion Nomograph .....	48
8. Limit Application Methodologies .....	49
9. Overview of Hardware and Data Flow .....	50
10. Tracking Plot of 1/rev Vibration for Consecutive Engine Starts .....	51
11. Vibration Amplitude as a Function of Inlet Pressure .....	52
12. Vibration Amplitude as a Function of Inlet Temperature .....	52
13. Vibration Amplitude as a Function of Lube Tank Pressure .....	53
14. Vibration Amplitude as a Function of Lube Tank Temperature .....	53
15. Response Amplitude Repeatability—Consecutive Decelerations .....	54
16. Response Amplitude Repeatability—Acceleration to Deceleration Variation at Constant Inlet Conditions .....	54
17. Bearing Health Characterization Algorithm Flow Chart .....	55
18. Sample Plots of Amplitude Versus K-Factor and Amplitude Versus Mode .....	56
19. Real-Time Bearing Health Monitoring Algorithm Flow Chart .....	57

## TABLES

<u>Page</u>	
1. Rolling Element Bearing Defect Frequencies .....	58
2. Characterization Algorithm Input File .....	59
3. Sample Statistical Output File .....	60

<u>Table</u>	<u>Page</u>
4. Sample Histogram .....	61
5. Fault Frequency Combinations and Diagnoses .....	61
6. Health Monitoring Algorithm Input File .....	62
7. CADDMAS Capabilites Versus HEMOS Requirements .....	64
NOMENCLATURE .....	65

## 1.0 INTRODUCTION

### 1.1 HISTORICAL BACKGROUND

By definition, monitoring is an act of extracting information from a system by observing instruments (sensing). Hence, online vibration monitoring consists of continuously acquiring vibration signals and using those reduced data as near real-time indicators of machine health. Figure 1 shows the three phases of a typical machinery deterioration versus run-time curve. Phase I is the run-in time; Phase II is the normal operation period; and Phase III is the failure development period. Early failure prediction sought by the online vibration monitoring system is designated by state "A" on the figure (Ref. 1).

The primary applications of online vibration monitoring programs have been in the paper, power, and chemical industries where relatively constant load operation of rotating machinery lends itself to near real-time monitoring. Continuous condition monitoring is a maintenance tool in these industries which allows predictive maintenance programs which are based on early warning. Here, the motive is to avoid unplanned shutdowns and minimize the cost of lost production (Ref. 1).

Importantly, detection of rolling element (ball or roller) bearing component faults, through vibration diagnostic techniques, has proven to be among the most reliable analysis tools for deducing mechanical faults in the relatively low-speed pumps, compressors, turbines, motors, etc. on which these industries rely (Refs. 2 and 3). Application of the principles of bearing fault diagnostics to high-speed turbomachinery such as aircraft turbine engines is, however, in its relative infancy (Ref. 4).

Implanted fault testing and post-mortem vibration analyses of bearing failures have shown that bearing fault diagnostics may also be successfully applied in aircraft turbine engines (Ref. 5). In some cases, post-failure analysis has uncovered indications of significant bearing faults minutes and even hours prior to catastrophic failure (Ref. 6). A dramatic example includes failure analysis of the bearing, shown in Fig. 2, in which the cracked cage, race, and rolling element faults were correctly diagnosed prior to engine teardown.

If the analyst's thought processes can be automated, then future bearing faults can be detected through online monitoring *before* a catastrophic failure manifests. The primary goal of the research reported herein is to develop such an algorithm.

Efforts involving determination of feasibility and preliminary requirements for an automated vibration-based online health monitoring system were conducted in S/T 147 project BC69EJ, Turbine Engine Durability. In FY93, the research effort was transferred to S/T



130 with the goal of developing the AEDC vibration-based Health Monitoring System (HEMOS) as an augmentation to the Computer Assisted Dynamic Data Monitoring and Analysis System (CADDMAS), project 0088. Efforts in FY93 focused on algorithm development for characterization and health monitoring based on bearing vibration. The ultimate goal of the HEMOS effort is to incorporate case, gear box, and frame-mounted vibration sensors, along with transient digital data, to survey overall health of the turbine engine test articles on test at AEDC.

## **1.2 STATEMENT OF PROBLEM**

Applied to machinery which operates at steady-state conditions for long periods, bearing fault diagnosis is a reliable, well-understood technique. In this case, developing faults tend to appear as changes to the vibratory response characteristics of the machine. The task of deciphering developing faults through vibration monitoring becomes much more difficult, however, when multistate variable operating turbomachines are involved. Aircraft engines by nature are extremely transient machines. Requirements to operate over a wide range of altitudes and flight velocities translate into an extensive matrix of inlet conditions (i.e., pressure, temperature, density, etc.). Since vibratory responses can vary significantly with one or more of these factors, a huge array of data may be required to define a baseline vibration signature for a specific engine model. A bearing health characterization algorithm is developed in Section 5.0 to accommodate this task in an offline mode.

The body of knowledge concerning bearing vibrations and related information has been investigated through an exhaustive literature survey. Two shortfalls which have been identified in the literature include:

1. Most published work is devoted to a particular bearing application on a specific machine.
2. Little work has been done to analyze the influence of bearing operating parameters on the vibratory environment.

This research effort addresses each of these shortfalls. First, the algorithm is adaptable by means of an input file to function for a variety of rolling element ball bearings in a number of different turbomachine applications. Second, influence of the primary bearing operating parameters on the bearing housing vibratory environment is analyzed. Identified trends are reported herein.

### 1.3 ENGINE OVERVIEW

Since much of the material presented is devoted to bearing vibrations in aircraft turbine engines, an overview of engine design and operation is presented. Many of the jet engines currently in use are of the turbofan design shown in simplified schematic form in Fig. 3.

These machines employ dual, concentric rotors. A low-pressure compressor or fan feeds compressed air to a high-pressure compressor (HPC) and a bypass duct. Air entering the HPC is further compressed before entering a combustion chamber (COMB) where fuel is injected, atomization transpires, and controlled combustion takes place. The hot exhaust gases are then expanded through a single or multistage high-pressure turbine (HPT). Further expansion then takes place through a low-pressure turbine (LPT) before mixing of the exhaust gases with the bypass air. The total mass flow is then exhausted through the tailpipe.

The HPC and HPT are connected via a shaft, and the combined assembly rotates at a speed (designated high rotor speed, NH) determined by design conditions and power setting. The high rotor assembly is generally supported by a forward-mounted ball element thrust bearing and an aft-mounted roller element radial bearing.

The fan and LPT are connected by a second shaft rotating at low rotor speed, NL, and similarly supported by two additional bearings. The low rotor shaft feeds through the high rotor shaft, and relative motion between the two shafts is constrained by an intershaft fifth bearing.

Due to space constraints within the engines, bearing vibration instrumentation is normally limited to radially oriented, housing-mounted accelerometers or velocity pickups. Rarely, proximity probes are employed through a housing penetration port to measure shaft displacement directly. Axially oriented vibration sensors are primarily used only on the engine outer case near the support frames since the concentric rotors inhibit access to the internal bearings. Also due to limited access, the intershaft bearing is seldom instrumented.

### 1.4 LIMITATIONS OF THE RESEARCH

The bearing health algorithm was developed for application to rolling element bearings in the diameter times running speed, DN, classification range from  $1.0 \times 10^6$  to  $1.8 \times 10^6$ . This classification generally encompasses most high-speed turbine engine ball element thrust and roller element radial support bearings. The algorithm is generic in nature, however, and could be applicable to much higher DN class bearings. Though automation of the algorithm

is outside the scope of this report, current plans for FY94 HEMOS work include automation of both the characterization and health monitoring algorithms. Preliminary vibration characterization of a single engine family and implementation of a prototype HEMOS are also planned.

Due to the widely varied conditions to which jet engines are subjected, analysis of vibration data to determine the effects of operating parameters was limited to data from a single vertically mounted bearing accelerometer operating over a range of speeds from idle to maximum power. Data from 21 different flight conditions were analyzed. Though the survey of vibration data was limited, several important conclusions may be drawn from the results (see Section 4.0).

The effort expended on the manual analysis points to the necessity for automating this process. A methodology for such automation is presented in Section 5.0 and will be automated in subsequent research.

It should also be noted that the algorithms developed herein rely on Fast Fourier Transformation (FFT) of vibration data. This technique is not adequate to capture bearing faults which occur during true *transient* conditions such as extremely high acceleration and deceleration rate maneuvers in turbine engines. Wavelet decomposition has been studied as a means of identification of bearing faults during such maneuvers (Ref. 7). The health monitoring algorithm should, however, identify fault symptoms during quasi-equilibrium conditions. Provided sudden, catastrophic failure does not occur during extreme throttle rate excursions, the health monitoring algorithm should be able to detect bearing faults once the machine has returned to a quasi-equilibrium state.

## 1.5 APPROACH

The research reported herein consisted of several phases. First, the bearing fault frequency equations were developed. Second, data analysis techniques for characterizing the vibratory responses measured at the bearing housing were designed. Next, an investigation of the effects of various machine operating parameters on the vibratory responses was conducted. Finally, a statistical approach was employed to ascertain bearing health criteria, and these criteria were incorporated into a functional algorithm which can be used in an automated monitoring capacity.

Phase 1 of the study developed the formulae for the bearing fault frequencies using kinematic analysis. Figure 4 illustrates the geometry and motion of a generic rolling element bearing (Ref. 8). The bearing fault frequency calculations are included in Table 1 (Ref. 2).

The fault frequencies, which include the fundamental train frequency (FTF), the ball spin frequency (BSF), ball passing frequency—outer race (BPFO), and the ball passing frequency—inner race (BPFI), are presented in Section 2.0.

Phase 2 of the research examined historical vibration data to determine the analysis techniques required for development of health criteria. Research activities reported include: (1) assessment of the most viable physical quantity of vibration (displacement, velocity, or acceleration) on which to base the algorithm, (2) determination of adequate means of data reduction and presentation (i.e., time domain, spectral plots, engine-order tracking plots, etc.), (3) results of an investigation to determine the primary bearing responses and the excitation source for each, and (4) development of two distinct modes of operation for the algorithm, including an evaluation of various data windows (i.e., start-up, coast-down, part-power, and maximum rotor speed) for incorporation into a data trending segment of the health monitoring algorithm.

Phase 3 of the study examined the influence of various operating parameters on the bearing vibratory response characteristics. Parameters which were found to have primary or secondary effects on the vibratory environment include operating shaft speeds, engine inlet pressure, engine inlet temperature, bearing lubrication pressure, and bearing lubrication temperature. Several important conclusions were drawn from this phase.

The final phase (Phase 4) incorporated a statistical approach to determine the relative health of lubricated rolling element bearings in high-speed turbomachinery for incorporation into the health monitoring algorithm. Figure 5 depicts a spectral response from an accelerometer mounted on a “healthy” bearing. The machine is operating at 6000 rpm (100 Hz). A once per revolution, 1/rev, response due to residual rotor unbalance is always present, as shown in the figure. Figure 6 shows a vibratory spectrum indicative of a deteriorated bearing. Presence of the FTF and modulation of running speed harmonics by the FTF usually indicate a worn or cracked bearing cage. Similar frequencies were evident in the spectra leading up to the bearing failure illustrated in Fig. 2. Other bearing faults can be deduced depending on the combinations of fault frequencies present (see Section 3.0). This phase of research developed an algorithm to statistically band the various vibratory response amplitudes and frequencies in an offline mode.

## **2.0 ROLLING ELEMENT BEARING FAULT FREQUENCIES**

In this section the bearing subcomponents are introduced, and the rolling motion within a bearing is discussed. The fundamental bearing fault frequencies are then developed through kinematic analysis of the rolling motion.

## 2.1 GENERAL—BEARING GEOMETRY AND MOTION

Rolling element bearings are used to support many different types of loads while providing a means of low-friction rotation or reciprocation within a machine. In the case of high-speed turbine engines, the two basic types of rolling element bearings include a ball element thrust bearing and a roller element radial support bearing. Relative motions within bearings are not restricted to simple movements (Ref. 8).

Referring again to Fig. 4, the bearing consists of four major subcomponents. The inner raceway or race is normally a groove in a shaft which has rotational speed,  $w_i$ . Likewise, the outer race is generally a groove in the bearing housing which provides for axial restraint and circumferential slip of the rolling element train. The outer race has rotational speed,  $w_o$ . The rolling element train consists of the rolling elements themselves constrained in relative position by a separator or cage, which also provides for bearing assembly. The train assembly rotates at rotational speed,  $w_m$ . The rolling elements have an absolute velocity made up of two components, including the rotational speed of the cage assembly and the relative rotational velocity of the elements with respect to the cage.

The contact angle,  $\beta$ , is defined to be the angle between a line perpendicular to the shaft axis and the line of action of the bearing force. For bearings having contact angles other than zero (i.e., other than simple radial support bearings), substantial spinning of the ball elements occurs simultaneously with rolling (Ref. 8).

Apart from the rotational speeds  $w_i$ ,  $w_o$ ,  $w_m$  and the contact angle,  $\beta$ , the relative motion between the bearing subcomponents is dependent only on the rolling element diameter,  $d_b$ , and the bearing mean or pitch diameter,  $d_m$ .

## 2.2 CAGE SPEED

In the case of heavily loaded bearings (such as those in turbine engines), the rolling element bearings can be analyzed without regard for dynamic effects. The motion can be described purely in terms of kinematics. Referring to Fig. 4, assume first that the inner and outer races are rotating at  $w_i$  and  $w_o$ , respectively. The velocity at a point on a rotating body in one dimension can be described by

$$v = w * r \quad (1)$$

where  $w$  is the rotational speed of the body, and  $r$  is the distance from the axis of rotation to the point (Ref. 8).

In the case of aircraft turbine engines, bearing vibration sensors (whether accelerometers, velocity pickups, or proximity probes) are oriented to pick up the radial component of vibration. The equations are, therefore, developed in terms of the radial components of vibration to be measured by these sensors. The radial velocity component at the inner race and ball element contact point will be

$$\begin{aligned} v_i &= w_i * r_i \\ v_i &= \frac{1}{2} * w_i * d_i \\ v_i &= \frac{1}{2} * w_i * (d_m - d_b \cos \beta) \end{aligned} \quad (2)$$

where  $r_i$  is the distance from the shaft center to the inner race surface. The velocity at the outer race contact point is

$$\begin{aligned} v_o &= w_o * r_o \\ v_o &= \frac{1}{2} * w_o * d_o \\ v_o &= \frac{1}{2} * w_o * (d_m + d_b \cos \beta) \end{aligned} \quad (3)$$

where  $r_o$  is the distance from the shaft center to the outer race surface. Introducing,

$$\mu = (d_b/d_m) * \cos \beta \quad (4)$$

and multiplying Eqs. (2) and (3) by  $1/d_m$ , respectively,

$$v_i = \frac{1}{2} * w_i * d_m (1 - \mu) \quad (5)$$

$$v_o = \frac{1}{2} * w_o * d_m (1 + \mu) \quad (6)$$

Assuming no relative slip, the velocity of the rolling element train may be taken as the mean of the inner and outer race velocities,  $v_m$ , such that

$$\begin{aligned} v_m &= \frac{1}{2} * (v_i + v_o) \quad \text{or,} \\ v_m &= \frac{1}{4} * d_m * \{w_i (1 - \mu) + w_o (1 + \mu)\} \end{aligned} \quad (7)$$

But,

$$v_m = \frac{1}{2} * w_m * d_m \quad (8)$$

Substituting Eq. (8) into Eq. (7) and solving for  $w_m$  yields

$$w_m = \frac{1}{2} * \{w_i (1 - \mu) + w_o (1 + \mu)\} \quad (9)$$

which gives an expression for the cage rotational speed in terms of the inner and outer race speeds and bearing geometry. Recognizing that

$w = 2\pi f$ , and substituting into Eq. (9) yields

$$f_m = \frac{1}{2} * \{f_i (1 - \mu) + f_o (1 + \mu)\} \quad (10)$$

which establishes the cage frequency,  $f_m$ , in cps with respect to a fixed reference frame (i.e., the vibration sensor).

### 2.3 ROLLING ELEMENT SPEED

To determine the rotational speed of the ball,  $w_b$ , we first introduce the angular speed of the cage relative to the inner race:

$$w_{mi} = w_m - w_i \quad (11)$$

Assuming no slip, the ball velocity,  $v_b$ , is identical to the velocity of the inner raceway *at the point of contact*. That is,

$$v_b = v_{mi} \text{ at the point of contact.} \quad (12)$$

But,

$$v_b = w_b * r_b = \frac{1}{2} * w_b * d_b, \text{ and} \quad (13)$$

$$v_{mi} = w_{mi} * r_{mi} = \frac{1}{2} * w_{mi} * d_m (1 - \mu) \quad (14)$$

Substituting Eqs. (13) and (14) into Eq. (12) gives

$$\frac{1}{2} * w_b * d_b = \frac{1}{2} * w_{mi} * d_m (1 - \mu) \quad \text{or,}$$

$$w_b = (d_m/d_b) * w_{mi} (1 - \mu) \quad (15)$$

Substituting Eq. (11) into Eq. (15) and again invoking

$$w = 2\pi f$$

$$f_b = (d_m/d_b) * (f_m - f_i) * (1 - \mu) \quad (16)$$

Substituting Eq. (10) into Eq. (16) for  $f_m$  yields

$$\begin{aligned} f_b &= (d_m/d_b) * (1 - \mu) * \left\{ \frac{1}{2} \{ f_i(1 - \mu) + f_o(1 + \mu) \} - f_i \right\} \\ f_b &= (d_m/d_b) * (1 - \mu) * \left\{ \frac{1}{2} f_i - f_i - \frac{1}{2} f_i \mu + \frac{1}{2} f_o(1 + \mu) \right\} \\ f_b &= (d_m/d_b) * (1 - \mu) * \left\{ \frac{1}{2} f_o(1 + \mu) - \frac{1}{2} f_i(1 + \mu) \right\} \\ f_b &= \frac{1}{2} * (d_m/d_b) * (1 - \mu) * (1 + \mu) * (f_o - f_i) \end{aligned} \quad (17)$$

Here, the frequency associated with the rolling element velocity relative to the cage has been determined. This is the frequency which may be detected by a vibration sensor in the event of a rolling element fault (Ref. 8).

## 2.4 SPECIAL APPLICATION

In the special case of a jet engine, most bearings have a stationary outer race and a rotating inner race. Thus,  $f_o = 0$  and Eqs. (10) and (17), respectively, reduce to

$$f_m = \frac{1}{2} f_i (1 - \mu), \text{ and} \quad (18)$$

$$f_b = -\frac{1}{2} (d_m/d_b) * (1 - \mu) * (1 + \mu) * f_i \quad (19)$$

The minus sign in Eq. (19) simply refers to the fact that the radial ball spin is opposite in direction relative to the cage rotation. Obviously, the vibration sensor will detect only the absolute frequency, or

$$f_b = \frac{1}{2} (d_m/d_b) * (1 - \mu) * (1 + \mu) * f_i \quad (20)$$

For a healthy bearing with proper clearance fit and no macroscopic defects, the vibration introduced by the cage and rolling elements contributes no significant amplitude, and vibration at  $f_m$  and  $f_b$  is masked by random vibration energy (i.e., *in the noise band* of the spectrum). The bearing fault frequencies will now be developed for the special case of a stationary outer race and rotating inner race as found in the turbine engines tested at the AEDC.



## 2.5 FUNDAMENTAL TRAIN FREQUENCY (FTF)

If the bearing is too loose or the cage is worn or cracked, discrete vibration amplitudes at  $f_m$  (FTF) and its harmonics may appear. If the defect is severe enough, the harmonics of running speed (i.e., multiples of  $f_i$ ) are modulated by FTF, and  $\pm$  sidebands of FTF will appear in the spectrum (cf. Fig. 6). So, the first bearing fault frequency has been derived for the special case of stationary outer race and rotating inner race.

$$FTF = f_m = \frac{1}{2}f_i(1 - \mu) \quad (21)$$

## 2.6 BALL PASS FREQUENCY—OUTER RACE (BPFO)

If there is a significant defect on the outer (stationary) race, then each rolling element produces an impact vibration as it rolls over the defect. The frequency which is generated by this phenomenon is related to the cage motion relative to a fixed reference frame. The vibration measured by the sensor will manifest at

$$BPFO = n * FTF = (n/2)f_i(1 - \mu) \quad (22)$$

where  $n$  is the number of rolling elements.

## 2.7 BALL PASS FREQUENCY—INNER RACE (BPFI)

If there is a defect on the inner (rotating) raceway, then a spike caused by the impacting of each rolling element as it contacts the defect again manifests as vibration. Note that the frequency of vibration in the fixed reference frame is due to the relative rotational speed of the inner race and the cage assembly such that

$$n * w_{\text{fixed}} = n * (w_i - w_m) \quad (23)$$

which reduces to

$$BPFI = n * f_{\text{fixed}}$$

$$BPFI = n * (f_i - f_m)$$

$$BPFI = n * (f_i - FTF) \quad (24)$$

Substitution for FTF gives

$$\begin{aligned}\text{BPFI} &= f_i - \frac{1}{2}f_i(1 - \mu) = \frac{1}{2}f_i + \frac{1}{2}f_i\mu \\ \text{BPFI} &= \frac{1}{2}f_i(1 + \mu)\end{aligned}\quad (25)$$

## 2.8 BALL SPIN FREQUENCY (BSF)

Finally, a single defect on a rolling element generates a measurable vibration at the relative spin frequency of the ball relative to the cage. Or, from Eq. (20),

$$\begin{aligned}\text{BSF} &= f_b = \frac{1}{2}(d_m/d_b) * (1 - \mu) * (1 + \mu) * f_i \\ \text{BSF} &= \frac{1}{2}(d_m/d_b) * f_i * (1 - \mu^2)\end{aligned}\quad (26)$$

with stationary outer race.

For the case of multiple rolling element defects, the frequency generated is simply a multiple,  $m * \text{BSF}$ , where  $m$  is the number of defects.

## 2.9 BEARING FAULT DIAGNOSIS

In the preceding sections, the bearing fault frequencies have been developed through an understanding of the relative motion between the bearing subcomponents and how they relate to a fixed observer (i.e., a radially mounted vibration sensor). A survey of the axial vibration is omitted since, in practical jet engine applications, clearances do not permit instrumentation of bearing housings mounted in an axial orientation. AEDC experience reveals that most bearing health-threatening defects may be detected through monitoring of the radial vibration alone.

Healthy bearings, in general, do not exhibit significant amplitudes of vibration at the bearing frequencies. When a defect is present, however, discrete responses can usually be detected at one or more fault frequencies. Initial presence of a measurable amplitude at a fault frequency above the spectral noise floor is analogous to detection of state "A" in Fig. 1. An experienced vibration analyst can usually track progression of worsening defects through changes in amplitudes and spectral content. Planned research activities will attempt to characterize this progression for incorporation into a health monitoring algorithm.

For the effort to date, however, the primary goal of the bearing health algorithm is to identify potential life-threatening defects as they initiate. If state "A" can be identified, then online operators may be able to take precautionary measures based on algorithm alarms.

### 3.0 DATA ANALYSIS TECHNIQUES

This section develops the data analysis techniques required to adequately characterize bearing vibration and implement a health monitoring algorithm. First, the quantities of vibration, (displacement, velocity, and acceleration) are discussed, and their interrelationships are examined. Second, data presentation alternatives are introduced. Third, the primary bearing responses are investigated, and limit application methodologies are discussed. Finally, a monitoring system overview is presented, and the continuous and trend modes are explained.

#### 3.1 PHYSICAL QUANTITIES OF VIBRATION

In the realm of vibration analysis, questions often arise concerning the most useful measured physical quantity for a specific application. Before looking more closely at various applications, the relationships between the physical quantities of vibration are examined. These quantities include displacement, velocity, and acceleration.

R. F. White makes a strong case for defining limits in terms of peak velocity (Ref. 9). He argues that velocity is proportional to the energy of vibration and is independent of frequency in the energy equation. He states that limits may be defined over a broader frequency range with less maximum-to-minimum deviation than displacement and acceleration limits. A development and analysis of the equations involved, however, leads to the conclusion that velocity alone is not satisfactory for a bearing health monitoring application.

Assuming steady-state sinusoidal motion of a body, the time-dependent displacement,  $D$ , is described as

$$D = B \sin (wt) \quad (27)$$

where the peak displacement,  $B$ , is in inches; the angular velocity,  $w = 2\pi f$ , is in rps; and frequency,  $f$ , is in cps or Hz. The velocity,  $v$ , may be taken as the derivative of displacement such that

$$\begin{aligned} v &= d/dt(D) = Bw \cos (wt) = 2\pi fB \cos (wt); \\ v &= 2\pi fB \sin (wt + 90) \end{aligned} \quad (28)$$

where the velocity is in in./sec (or ips). The acceleration,  $a$ , is the derivative of velocity such that

$$a = d/dt(V) = -B\omega^2 \sin(\omega t)$$

$$a = (2\pi f)^2 B \sin(\omega t + 180) \quad (29)$$

where acceleration is expressed in in./sec<sup>2</sup>.

Recognizing that the sinusoidal phase shifts in Eqs. (27), (28), and (29) simply refer to the fact that velocity leads displacement by 90 deg and acceleration leads displacement by 180 deg, examine the relationships between the peak values of displacement, velocity, and acceleration.

Setting  $\omega t = 0$  deg in Eq. (28) yields the relationship between peak velocity and peak displacement:

$$v = 2\pi f B \text{ or } B = v / (2\pi f) \quad (30)$$

where  $v$  is now peak velocity (ips pk).

Setting  $\omega t = 270$  deg in Eq. (29) yields the relationship between peak acceleration and peak displacement:

$$a = (2\pi f)^2 B \text{ or } B = a / (2\pi f)^2 \quad (31)$$

where  $a$  is now in in./sec<sup>2</sup> peak.

Equating the right halves of Eqs. (30) and (31) yields the relationship between peak acceleration and peak velocity:

$$a = 2\pi f v \text{ or } v = a / 2\pi f \quad (32)$$

Now, introduce 1 mil = 0.001 in., and 1 g = 386.087 in./sec<sup>2</sup> at sea level. These units of displacement and acceleration, respectively, are much friendlier for application to vibration theory.

Further, define  $d = 2B$  to be the peak-to-peak displacement of the body. On proper substitution and conversion, the relationships in Eqs. (30), (31), and (32), respectively, become:

$$d = 318.3 * (v / f) \text{ or } v = df / 318.3, \quad (33)$$

$$a = (f / 139.85)^2 * d \text{ or } d = (139.85 / f)^2 * a, \quad (34)$$

$$a = (f * v) / 61.43 \text{ or } v = 61.43 * a / f \quad (35)$$

By looking at these simplified equations, we get an intuitive feel for which units (and thereby which types of sensors) are most useful for different applications. Note that most amplitudes of vibration in high-speed turbomachinery range from 0 to 10 mils peak to peak (pk-pk), 0 to 0.5 ips peak, and 0 to 20 g's peak.

In Eq. (33), note that displacement and velocity become equal at  $f = 318.3$  Hz, suggesting that as frequency increases far above 318 Hz, displacement measurements grow smaller and smaller for constant velocity. At  $f \approx 1600$  Hz, measured displacement is less than 1 percent of the maximum full-scale range of expected vibration. As such, most sensors are unable to resolve discrete displacement components at higher frequencies. Conversely, vibrations at much lower frequencies ( $f \leq 2$  Hz) render the velocity spectrum nearly useless, and displacement amplitude resolution is far better.

Similarly, Eq. (34) shows that acceleration and displacement become equivalent at  $f \approx 140$  Hz. Much smaller displacements become significant at higher frequencies for constant acceleration (due to the  $f^2$  term), and units of acceleration are preferable at frequencies above 800 Hz. Equation (35) indicates that velocity and acceleration become equivalent at  $\approx 61$  Hz. At frequencies greater than approximately 1200 Hz, vibration responses indicative of a rolling element fault are *in the noise band* of the velocity spectrum, but discrete peaks indicative of race faults are discernible in the acceleration spectrum.

To examine the effects of frequency on amplitude of displacement, velocity, and acceleration more closely, examine the nomograph in Fig. 7 and consider the following example. Point P in the figure is plotted at a vibratory frequency of 8 cps or Hz. Displacement amplitude is 4 mils pk-pk; velocity amplitude is 0.09 ips pk; and acceleration amplitude is 0.01 g's pk. By generally accepted guidelines, 4 mils pk-pk is relatively alarming; 0.09 ips pk is fairly benign; and 0.01 g's pk is of little concern. The analyst must discern the excitation source for the response and determine its potential impact to the rotating machine. Importantly, a 4 mils pk-pk displacement response at the FTF identifies a bearing nearing catastrophic failure, whereas an acceleration of only 0.01 g's pk likely lies within the noise band of the data.

Point Q in Fig. 7 illustrates a converse situation. At 10,000 cps, displacement amplitude is 0.002 mils pk-pk; velocity amplitude is 0.065 ips pk; and acceleration amplitude is 10 g's pk. In this case, velocity and displacement amplitudes warrant no particular concern, whereas acceleration energy is at the danger level. Frequency has an obvious effect on the amplitudes

of response, and the analyst must take into account the physical quantity of vibration (displacement, velocity, or acceleration) before concluding relative machine health.

Since the class of high-speed turbomachinery investigated herein has bearing fault frequencies which vary from approximately 30 Hz to 2000 Hz, it seems prudent to adapt the algorithm to take advantage of all vibration quantities: displacement, velocity, *and* acceleration.

Experience in analyzing vibration data from turbine engine bearings suggests the following frequency ranges for the physical quantities of vibration are an acceptable guideline:

displacement – 0 to 500 Hz,

velocity – 200 to 1200 Hz, and

acceleration – 800 to 10,000 Hz.

In addition to the theoretical development and inherent advantages, there is a very good practical reason for taking this approach. All jet engine manufacturers do not use similar vibration sensors. Proximity probes measuring displacement, velocimeters measuring velocity, and accelerometers measuring acceleration are all used in some applications for determining the engine vibratory characteristics.

### **3.2 DATA PRESENTATION ALTERNATIVES**

The AEDC vibration-based HEMOS, when fully developed, should be capable of providing all usual vibration data presentation formats including (but not limited to): spectra, trending plots, engine-order tracking plots, waterfall plots, Campbell diagrams, orbits, Bode' plots, Nyquist plots, tables, alarm synopses, etc. (Ref. 6). For primary health monitoring purposes, however, modified spectra of vibratory amplitude versus K-Factor and amplitude versus vibratory mode are used. This approach is explained in detail and justified later in this section.

### **3.3 PRIMARY BEARING VIBRATORY RESPONSES**

To ascertain the most likely responses of bearings to vibration stimuli in jet engines, recall the engine description introduced in Section 1.3 and examine the purpose of the bearings. Rolling element bearings in these high-speed turbomachines are required to provide smooth operation of the rotor shafts and to transfer unwanted energy in the form of vibration out of the machine through the support frames.

Based on the overall assembly, some primary response frequencies can be surmised. Since all rotating assemblies have some residual unbalance due to manufacturing tolerances, material flaws, etc., each of the bearings responds to a 1/rev excitation, and this response is measured by a sensor due to passing of the rotor's *heavy spot* (attributed to residual mass unbalance, i.e., eccentricity). The frequency of vibration occurs at rpm/60. Since the two rotors rotate at different speeds, it can be safely assumed that the high rotor support bearings will primarily respond at 1/rev of the high rotor shaft (1X NH), and the low rotor bearings will respond at 1X NL. Depending on the energy of vibration and shaft alignment within the bearings, harmonics of the 1X responses may also occur at 2X, 3X, etc.

Since a path of vibration transmissibility between the two shafts exists in the form of the intershaft bearing, the thrust and radial support bearings of the low rotor will likely respond (to a lesser degree) to the 1X NH stimulus, and the high rotor bearings will respond (to a lesser degree) to the 1X NL excitation.

The above responses are deemed to be *normal* and provided they are within acceptable limits, pose no threat to the turbomachine hardware. There are other responses, however, which indicate potential health hazards to the engine (R. L. Eshelman, "Machine Diagnostics," Vibration Institute: Machinery Vibration Analysis I, Course Notes, Nashville, TN, November 17-20, 1987). Such responses include:

1. Extreme 1X NH or NL due to a bowed or bent rotor,
2. Significant 2X NH or NL attributable to a shaft which is severely misaligned in its bearings,
3. Subsynchronous vibration at 0.4X to 0.48X NH or NL indicative of an oil whirl phenomenon,
4. Any of the bearing fault frequencies described in Section 2.0 which betray the presence of localized defects within the bearing,
5. Vibration at 0.5X NH or NL and due to seal rubs, blade tip rubs, or coupling looseness,
6. Extreme vibration at 0.25X or 0.33X and harmonics due to a subsynchronous resonance (oil whip),
7. Sum and difference (beat) frequencies such as (NH – NL) or (NH + NL) which excite damaging hardware resonances, and

8. Rarely, vibration at a known blade-passing frequency which excites a frame strut aeromechanical resonance (Ref. 6).

Now that an understanding of the hardware assembly and the primary expected bearing response frequencies has been developed, an important insight into the duties which can befall a bearing health monitoring algorithm is gained. An investigation of two limit application methodologies follows.

### 3.4 METHODOLOGIES FOR LIMIT APPLICATION

Because of the transient nature of aircraft engines, a methodology was needed for comparison of vibratory responses to established limits. To investigate further, a *typical* turbofan engine with a low rotor operating speed regime of 3000 to 6000 rpm was considered (Fig. 8 and Ref. 6). At 3000 rpm (Fig. 8A, top), a 1X response of 2 mils pk-pk at 50 Hz (3000 rpm) and a 2X response of 1 mil pk-pk at 100 Hz would be indicative of a relatively rough running rotor (2 mils 1X at idle) with bearings that are poorly aligned to the shaft.

When accelerated to 6000 rpm (Fig. 8A, lower), a 1X response of 2 mils pk-pk occurs at 100 Hz (6000 rpm), and no significant 2X component of vibration was noted. This response characteristic represents a healthy engine which is operating well within the vibration limits of most manufacturers.

In the first case, a 100-Hz response of 1 mil pk-pk was interpreted as a fault (bearing misalignment); in the second case, a 100-Hz response of 2 mils pk-pk was deemed to be *normal*. Consequently, the limit application methodology in a turbine engine vibration monitoring system must be able to recognize the various responses in the spectrum and apply the appropriate limits, suggesting a *sliding mask* limit application technique where a limit envelope (or mask) must change with changing speeds. Theoretically, a different limit mask exists for every combination of low and high rotor speeds, and an expert system is required to continuously identify the significant spectral responses and apply the appropriate limits. The limit mask must slide to the right in the frequency domain as the engine is accelerated from 3000 rpm (Fig. 8A, top) to 6000 rpm (Fig. 8A, lower).

By employing the *K-Factor* approach to the limit application illustrated in Fig. 8B, the problem becomes greatly simplified. The K-Factor approach draws on the fact that all rotor dynamic responses are related to rotor speed in an integral or nonintegral manner, such that

$$f = \text{K-Factor} * N / 60$$

or,



$$\text{K-Factor} = f * 60 / N$$

where N is high or low rotor speed, NH or NL, and K-Factor is a constant related to geometry or phenomena.

For integral vibrations, the K-Factor is simply an integer multiple of engine speed. For nonintegral vibrations, K-Factor is a mixed fractional number (i.e., K-Factor  $\approx$  0.47 for vibration due to oil whirl phenomenon). These responses are easily computed, so if the nominal response range for a given engine family can be characterized in terms of amplitude versus K-Factor, then the bearing algorithm can be programmed to interrogate for potential problems using a single limit mask and avoid the huge development task associated with a sliding mask (Ref. 6).

The selection of the K-Factor approach to limit application is a potential means of avoiding one of the major pitfalls of automated health monitoring systems: false alarms. By separating the vibratory responses associated with NH and NL for each sensor's data stream, confusion over which responses are nonsynchronous (and thus potential fault indications) may be avoided.

Yet another limit application is required due to the nature of modal vibration. In some cases (e.g., a bearing housing resonance), vibrations occur across the speed regime at near constant frequency. This form of vibration results in a *smearing* effect in the amplitude versus K-Factor spectrum. Therefore, the algorithms must take into account known modal responses, and alert and alarm limits must be established into a limit application methodology. The means by which this form of vibration is handled by the algorithms is discussed more fully in Section 5.0.

### 3.5 MODES OF ALGORITHM OPERATION

To avoid confusion with vibratory modes of the engine components, the bearing health monitoring algorithm has two separate, parallel modes of operation. First, the *continuous* mode of the algorithm acts as a watchdog for potential hardware faults as they initiate and develop. The *trend* mode screens acquired data during special user-defined "windows" of operation to quantify overall rotor system degradation and potential faults which manifest, but may not exceed the limits imposed in the continuous mode of operation. An overview of the hardware involved and the data flow is shown in Fig. 9 (Ref. 6).

In the continuous mode, acquired vibration and transient digital data are continually merged and passed to a host computer system where the monitoring algorithm may be applied to the processed data. The transient digital data include engine rotor speeds (NH and NL),

lube oil pressures and temperatures, and inlet conditions (altitude, Mach number, pressure, temperature, density, etc.). The continuous mode of the algorithm checks vibrations versus manufacturer's specified limits and screens for potential rotor dynamic and bearing faults. If no potential problems are identified, the merged data remain in a circular file to be overwritten. Should a potential problem be identified, however, an alarm system identifies the channel(s) in an overlimit condition, and the data from all channels are written to a file for permanent storage. In the case of an alarm condition, the circular file data are also dumped immediately to permanent storage to provide a 20-min history of the engine conditions leading up to a fault. A user interface is provided to: (1) input necessary information for the algorithm and (2) allow interaction for user interrogation of the permanent storage file. The continuous mode is operational whenever the engine is rotating (Ref. 6).

Before discussing the *trend* mode of algorithm operation, a practical example is required to examine the need for such a mode. On shutdown following a turbine engine test, a seal rub apparently took place along a rotor shaft. Localized heating occurred and resulted in a permanent set (bow) of the shaft. On start-up for the next test period, the engine accelerated to idle speed without encroaching on a manufacturer-specified vibration limit. As the engine was accelerated toward maximum power, however, extreme vibration was noted, and the engine was shutdown immediately. Unfortunately, significant damage occurred before the shutdown was ordered.

As shown in Fig. 10, post-event analysis indicated that a major shift in rotor critical speed of approximately 250 rpm and maximum attained amplitude had occurred between consecutive starts of the engine. Through investigation of these data *windows*, it became obvious that a major shift in rotor dynamics had taken place. If a trend mode algorithm had been in place, the changes would have been recognized, and the hardware damage induced on engine acceleration toward maximum power may have been avoided.

The trend mode of the algorithm is invoked on user demand to provide a historical data trending capability during defined data *windows*. Potential windows may include engine starts/shutdowns, 2-min accelerations and decelerations at health check flight conditions, baseline vibration data at maximum power, etc. Each of these windows is chosen to identify shifts in rotor dynamic characteristics and to quantify engine deterioration in a further effort to identify state "A" (initiation of hardware faults) shown in Fig. 1. The trend data software should compute statistical variations of current data with the historical database and generate a user-specified hardcopy comparison or CRT display for the vibration analyst(s). The trend mode allows visibility of pertinent trend information for all channels on user demand without interrupting the flow of data through the continuous mode of the algorithm. A user interface is again necessary to specify input files, output format, and data window start/stop times (Ref. 6).

Detailed development of the continuous and trend modes of the real-time health monitoring algorithm is presented in Section 5.5.

## **4.0 ANALYTICAL RESULTS**

This section relates results of analysis conducted on response characteristics from a single bearing housing-mounted accelerometer. First, the effects of bearing operating parameters on vibration characteristics are examined. Second, the repeatability of response amplitudes are compared during back-to-back decelerations and consecutive acceleration-to-deceleration throttle movements at similar flight conditions. Finally, the necessity for automating the analysis process is discussed.

### **4.1 BACKGROUND**

Before an expert system can be programmed to identify abnormal conditions based on vibratory spectra, normal vibratory responses must first be characterized. Analysis was conducted using reduced vibration data from a typical air-breathing turbofan engine. This engine was determined through analysis and teardown inspections to have no abnormal rotor dynamic wear or degradation. The goal of this analysis included identifying the engine operating parameters which have primary or secondary effects on the vibratory characteristics of various engine components.

To limit the scope of effort, data from a single accelerometer were reduced and analyzed manually. This vertically oriented sensor was chosen because it was the most responsive accelerometer to internal vibrations. For simplicity, the bearing-mounted accelerometer is designated B-VIB.

### **4.2 OPERATING PARAMETER EFFECTS ON VIBRATIONS**

Preliminary investigation showed that several engine operating parameters influenced the vibratory response characteristics measured. The primary response measured was always the 1/rev signal generated by the residual unbalance of the high rotor (core) system. As noted in Section 3.0, this was expected since the B-VIB sensor was mounted on the axial thrust bearing of the high rotor system. The function of this bearing is to restrain forward thrust-transmitting unbalance energy out of the engine in the form of vibration through the frame struts. Vibration amplitudes measured by B-VIB appeared to decrease with increasing inlet pressure (Fig. 11), and the 1/rev response increased with increasing inlet temperature (Fig. 12). These data were fitted using least squares curve-fit methods. Further investigation into these trends, however, yielded an important result (Ref. 6).

At each of the two higher inlet pressure conditions shown in Fig. 11, the engine was operating at a control-specified pressure limit, and low rotor (fan) speed had been decreased to maintain engine operation at this limit. Since the fan rotor and core rotor were aerodynamically coupled, this resulted in a lower core speed as well. The result is a lower vibration amplitude measured at the bearing housing, because the residual mass unbalance is rotating at a lower speed at higher inlet pressures (for identical power settings).

Data trends in Fig. 12 indicate increasing vibratory amplitude with increasing inlet temperature for three different inlet pressures. Once again, these trends are actually related to NH. The fan speed schedule for most turbofan engine families is primarily a function of inlet temperature subject to various pressure, temperature, and speed limitations. Fan speed increases with increasing temperature (until limits are incurred), aerodynamically driving core speed higher as well.

Similar trends held for lube oil pressure and temperature, as shown in Figs. 13 and 14, respectively. Vibration amplitude increased with increasing lube tank pressure (Fig. 13), but further investigation revealed that this trend was also primarily related to speed. The constant volume lube pump was driven by the core shaft through the power take-off (PTO) shaft and gearbox. Consequently, higher core speeds resulted in higher pump speeds and higher lube tank pressures. Vibrations once again increased with increasing core speed. Likewise, lube tank temperature had a secondary effect on vibration amplitude (Fig. 14). Increasing vibration with increasing lube temperature was again related to core speed through the gearbox (Ref. 6).

Although several parameters were found to have a secondary effect on vibrations measured by B-VIB, the primary effect was always due to core rotor speed. In the absence of operation at a critical speed (which is generally designed to be outside the engine operating regime), the highest vibratory amplitudes are expected at the highest speeds and may be attributed to residual mass unbalance in the rotor. This is a significant conclusion, because if broadly applicable, it greatly simplifies the approach necessary to monitor bearing health (Ref. 6).

If the normal range of vibratory amplitudes can be identified for each family of engines, then it should be possible to screen for abnormalities based on 1/rev vibration and its harmonics. Planned HEMOS efforts for FY 94 will attempt to characterize this normal range of vibration statistically for a single engine family. Addition of a capability to calculate and screen for the bearing fault frequencies will supplement the 1/rev monitoring, and a bearing health monitoring scheme can thus be implemented via the bearing algorithm.

Engine manufacturers have well-developed limits for 1/rev NL and NH, and incorporation of these limits into the monitoring methodology will be simple. Though more complicated,

expected resonant crossings for various components, caused by acoustic or wake shedding excitation, may be computed. Parametric studies should be conducted to determine the range of response magnitudes attributable to such resonances. For example, high vibratory stresses in support frame struts sometimes induce vibratory responses measured at bearings. Provided the algorithm is programmed to expect these resonances and associated increase in vibrations, false alarms will be kept to a minimum. Again, the difficulty lies in characterizing the expected range of amplitudes for each resonant response, and further analysis is required.

### **4.3 RESPONSE AMPLITUDE REPEATABILITY**

A representative plot of the variation in response amplitude versus frequency for the B-VIB accelerometer is included as Fig. 15. For consecutive decelerations at similar inlet conditions, B-VIB variation ranged from 0 to 8 percent for measured responses above the noise floor. Similar variations were noted at other flight conditions as well (Ref. 6).

An investigation of acceleration/deceleration response amplitude variation was also conducted (Fig. 16). Variations ranged from 0 to 22 percent for B-VIB. Due to significant differences in bearing loads between acceleration and deceleration operation in some engine families, further analyses are necessary to glean meaningful results for incorporation into the algorithm (Ref. 6).

### **4.4 NECESSITY FOR AUTOMATION**

The analysis results reported herein were a significant undertaking. Limiting the effort to one data channel for a minimal number of engine data acquisition events allowed certain trends and conclusions to be drawn, but much is yet to be learned. Couple this level of effort with the fact that output from one accelerometer at 21 flight conditions (accelerations/decelerations at each) was analyzed, and one begins to see the enormity of analysis required to characterize the vibration responses over the flight map. The necessity for automating the analysis process becomes apparent when it is realized that many turbofan test engines are equipped with up to 12 bearing accelerometers, and many test programs encompass 50 to 60 flight conditions (Ref. 6).

The bearing health characterization algorithm will first be applied to offline data. A database of expected vibratory responses will be acquired for several test engine families. Capabilities to statistically characterize the range of bearing vibratory responses were developed and are discussed in the next section.

## 5.0 BEARING HEALTH CRITERIA AND MONITORING

As stated previously, the quest to identify faulty hardware components through automated vibration monitoring must begin with the characterization of *healthy* hardware. The goals of this section include: (1) development of a bearing health characterization algorithm, (2) examination of the role of operating environment on the vibration characteristics, (3) examination of the significance of combinations of fault frequencies in fault diagnosis, and (4) a discussion of the actual real-time bearing health monitoring algorithm and its decision-making process.

### 5.1 BASELINE VIBRATION CONSIDERATIONS

Manufacturing and assembly tolerances can stack up to yield slightly different vibration characteristics between even consecutive serial number engines in the same family. Slight variations in bearing stiffness and alignment can influence the magnitude and speed at which rotor dynamic resonances (critical speeds) occur. Further, balancing of individual rotor bladed disks and subsequent stacking can yield differences in the amplitude of 1/rev vibration and its harmonics for engines in the same family. Finally, control tolerances and mechanical looseness in variable geometry can change mass flow and aerodynamic loading for similar engines at like flight conditions and result in slightly different vibration characteristics. For these reasons, it is obvious that each family of air-breathing engines requires a statistical *banding* to identify the full regime of healthy vibration characteristics over the entire engine operating envelope. The following algorithm was developed to provide such a characterization.

### 5.2 BEARING HEALTH CHARACTERIZATION ALGORITHM

Figure 17 illustrates the logic flow for the automated health characterization algorithm. Although this discussion is limited to bearing-mounted vibration sensors, the algorithm may be used to statistically characterize any engine-mounted vibration sensor. This algorithm is used in an offline mode to develop limits which may then be applied in the online health monitoring algorithm. Referring to the numbered steps in Fig. 17, this section addresses each division in the logic flow process.

Initially, data are read from an individual data channel. The data are first checked to verify that incoming overall signal levels do not exceed the maximum voltage level obtainable with the data conditioning equipment in use (Step 1). Generally, this is a maximum of 1.414 volts rms for our application. If a response level exceeds the maximum due to an open, noisy channel, then the data are immediately omitted from consideration in the characterization process.

Next, Fast Fourier Transformation (FFT) of the time domain data is accomplished for the entire data event (Step 2). An event is typically a slow ( $\approx 2$  min) acceleration or deceleration or a health check point at steady-state operating conditions (i.e., speed, inlet conditions constant). The data are then temporarily stored as a succession of 1024 point ensembles. The usual digitization process using a Zonic model 6080 analog-to-digital conversion processor achieves about 2.5 ensembles per second of time domain data, though CADDMAS capabilities discussed later in this section should provide gapless data at 100 ensembles per second.

An input file is then read by the computer (Step 3). The input file includes a breakdown, by engine component, of all data channels. Each parameter is assigned a dynamic number, and each component includes one or more dynamic numbers. A switch, NSW, is included to tell the program whether a component is more susceptible to high rotor or low rotor excitation. For example, a No. 3 bearing accelerometer is more likely to respond primarily to high rotor excitation since this bearing is the thrust bearing for the high rotor system.

Other information in the file includes known modal responses measured by each vibration sensor. A housing resonance may exist, for instance, at approximately 750 Hz. Another key input includes frequency ranges indicative of line noise (e.g., 60 Hz TVA or 15 Hz cable whip). An example input file is included as Table 2.

For each ensemble frequency, responses above a designated threshold are screened for noise content as defined in the input file (Step 4). Any response occurring at a noise frequency is automatically deleted from further interrogation.

K-Factors are then computed for each spectral response over a designated threshold level according to the following hierarchy (Step 5):

$$\text{NSW} = \text{NH}, \text{ then } K_i = f_i * 60 / \text{NH}$$

or, if

$$\text{NSW} = \text{NL}, \text{ then } K_i = f_i * 60 / \text{NL}$$

For simplicity, assume that  $\text{NSW} = \text{NH}$ . Each  $K_i$  is compared against multiples of high rotor speed (i.e., 1X NH, 2X NH, etc.). If a match is found, then that response is categorized according to its engine-order multiple, and all associated data ( $A_i$ ,  $f_i$ ,  $K_i$ ,  $\text{NH}_i$ ,  $\text{NL}_i$ , etc.) stored in an array (Step 6). Once the data have been categorized at any point throughout the logic process, then they are omitted from further consideration. (In some engines, extreme vibration may occur due to a combination of excitation sources such as 1X NH = 2X NL. Additional logic may be necessary for these special cases.) Unmatched responses at this point have new K-Factors computed based on low rotor speed, and the comparison process is

repeated in an effort to decipher responses associated with low rotor excitation. Matched responses are thereby categorized and stored. Unmatched responses continue through the logic.

Rotor dynamic responses related to rotor speed excitations are by far the most common. Further, any modal responses are likely to reach maxima at engine-order crossings. Consequently, the most important characterization information is gleaned through the K-Factor calculation and interrogation process.

Unmatched spectral responses after the K-Factor matching process are next interrogated for modal frequency content based on the input file information (Step 7). If a response above the threshold falls into a frequency and speed regime defined in the input file, that response is categorized, and pertinent data are once again stored. Unmatched responses are passed on to the next phase of interrogation.

Beat (or sum and difference) frequency responses are fairly common in two-rotor systems. Based on AEDC vibration experience, primary beat responses occur at frequencies in Hz of  $(NH - NL) / 60$ ,  $(NH + NL) / 60$ , and/or  $(NH + NL) / 120$ . Step 8 in the algorithm searches for beat frequency responses and stores pertinent information accordingly.

The goal of the execution is to categorize as many of the spectral responses possible for each ensemble of data that is passed through the algorithm. Virtually all real-world dynamic systems include random energy responses, however. Unmatched responses at this point in the algorithm are classified as random, and each amplitude, frequency,  $K_i$ , NH, NL, etc. is stored in a separate array (Step 9).

Step 10 in the algorithm computes and stores running average, maxima, minima, and standard deviations for all K-Factors and modal frequencies, respectively. Once complete, the next ensemble of data is read in, and the process starts over again. When all ensembles have been analyzed by the automated routine, the next data parameter is introduced and processed.

After all parameters in a data set have been characterized, the algorithm produces three output items which are key aides in determining appropriate limits for the actual real-time health monitoring algorithm (Step 11). These outputs include:

1. A table of statistical parameters for each vibration sensor characterized,
2. A histogram indicating the number of characterized responses as a percent of maximum amplitude, and



### 3. Plots of amplitude versus $K_{NH}$ , $K_{NL}$ , and $Mode_i$ .

Table 3 is an example of statistical output for a single parameter, and Table 4 illustrates a sample histogram.

Figure 18 illustrates the proposed combined plot format. In the amplitude versus K-Factor plot at left in Fig. 18, rotor dynamic related responses, which have been identified by the characterization algorithm, are shown. Minima, maxima, and averages are indicated for all identified vibration responses above the specified threshold. The dashed line in this plot indicates a potential limit mask based on the data scatter and standard deviation data. Similar information for vibratory mode-related responses is shown at right in Fig. 18.

Once the characterization is complete for all sensors installed on a turbine engine, meaningful limits can be established for each family of engines for incorporation into the health monitoring algorithm discussed later in this section.

## 5.3 ROLE OF OPERATING ENVIRONMENT

In Section 3.0, it was concluded that the primary excitations of a single thrust bearing were directly related to running speeds. Still, the turbine engine is a transient machine by nature, required to operate over a multitude of extremes. With the newly developed automated characterization algorithm, further work can be accomplished in determining potential influences of pressures, temperatures, variable vane angles, viscosity, density, etc. on the rotor dynamic characteristics of the various machines.

Results of this further analysis can be incorporated into the algorithms as necessary to optimize the health monitoring capability.

## 5.4 FAULT FREQUENCY COMBINATIONS

The characterization algorithm allows assessment of amplitude versus K-Factor and amplitude versus mode limits which may be incorporated into the health monitoring algorithm, as illustrated in Fig. 18. These limits should be specified to maximize the fault detection capability while minimizing incidence of false alarms. A healthy bearing should exhibit no fault frequency responses above the established noise floor (i.e., the established random energy of vibration at these frequencies). Appearance of significant amplitudes at K-Factors related to these frequencies indicates a developing fault.

R. L. Eshleman developed a table of fault frequency combinations and the associated hardware faults, "Rolling Element Bearing Analysis," Vibration Institute: Machinery

Vibration Analysis I, Course Notes, Nashville, TN, November 17-20, 1987. This information is paraphrased in Table 5. Although the primary goal of the health monitoring algorithm is to alert engine operators of any potential hardware problem, the end-product monitoring system may well include a probable diagnosis based on the fault conditions identified.

## 5.5 REAL-TIME BEARING HEALTH MONITORING ALGORITHM

Figure 19 illustrates the logic flow process incorporated into the real-time bearing health monitoring algorithm. Similar to the characterization algorithm, each step in the decision-making process is labeled and discussed.

The initial step after data acquisition and conditioning is to apply a method of checking for spurious data (Step 1). This is likely to be a combination of checking for a saturated channel and interrogating the user-defined noise frequency bands (as accomplished in the characterization algorithm). Every effort is made to minimize false alarms, since such occurrences degrade user confidence in the system.

The data are digitized and FFT-processed (Step 2). Care should be taken, however, to preserve a peak-to-peak voltage,  $V_{pk-pk}$ , as an indication of the overall vibration level from each vibration sensor.

As in the characterization algorithm, the health monitoring process requires that a user-specified engine data file be read (Step 3). This file includes information such as engine type and model, engine serial number, thresholds, pertinent component geometries, accelerometer locations, vibration parameter names and numbers, baseline vibration data from a historical database (discrete and overall), previous trending data windows, specific amplitude versus K-Factor and amplitude versus mode alert and alarm limits, and other pertinent information. This data file is used by both continuous and trend modes of the monitoring system and must be read in at this point in the logic process. A sample input file is included as Table 6.

Overall vibration, 1/rev NL, and 1/rev NH responses are then screened versus specified manufacturer's vibration limits (Step 4). The 1/rev NL and NH responses can be preserved using digital filtering techniques. If a warning or alarm limit is surpassed, a *yellow* or *red* alarm is initiated and data from all channels downloaded into permanent file storage. This act does not stop the continued flow of data through the logic.

Assuming the online vibration monitoring personnel have requested a trending profile, the following constraints are specified in Step 5:

1. The pertinent database to use for comparison,
2. The data window about to be executed (i.e., a 30-Kft and 0.9 Mach number acceleration),
3. The vibration channels of interest, and
4. The output format desired.

The system next computes and displays the overall, 1X NH, and 1X NL responses versus speed or time (Step 6). The baseline signatures are displayed as background data, and allowable standard deviation from the input file indicates a range of allowable data scatter about the baseline. The user should be able to interface with the system and scroll through the trending data plots for all sensors specified.

The trending system then computes a *norm* which is an indication of the deviation of the current signature from the historical baseline and previous trend data for the current test article and vibration sensor (Step 7). Mathematically rigorous comparative functions are incorporated to compute the *norm* (Ref. 10).

The trending capability also includes hardcopy output of trend and comparison data in a user-specified format within 5 min after the data acquisition is complete. This completes specifications for the trending logic flow, and the parallel logic for the continuous mode follows.

The next step in the continuous mode logic (Step 8) computes and stores the K-Factors associated with all frequencies in the spectra that have amplitudes above a specified threshold or noise floor. These computed K-Factors are designated  $K\text{-Factor}_{\text{calc}}$ . As specified in the characterization routine, these K-Factors can be a function of NH and/or NL. For brevity, only a single rotor speed, N, is introduced.

For I = 1 to L

$$K\text{-Factor}_{\text{calc}}(I) = (\text{freq}(I) * 60) / N$$

Next I

where L is the number of frequencies in spectrum above specified amplitude threshold, and N is high or low rotor speed.

The next step is a comparison to identify those  $K\text{-Factor}_{\text{calc}}$  that have a match in the baseline amplitude versus  $K\text{-Factor}$  limit methodology (Step 9). Each identified response is compared to established limits. If a limit has been exceeded, a *yellow* or *red* alarm is initiated, and the data from all channels are dumped to a permanent storage file. The initiation of any alarm does not stop the flow of data through the logic.

If at any time during the logic flow process all responses above the threshold level are not matched with alert or alarm conditions, the data simply pass to the circular file to be overwritten. As long as unmatched responses do exist, however, the data interrogation continues.

Similar to the methodology introduced in the characterization algorithm, Step 10 interrogates unmatched spectral responses versus the modal response frequency regions specified in the input file. When matches are found, the amplitudes are compared with established limits. If alert (yellow) or alarm (red) limits are exceeded, the data are dumped to permanent storage, and the engine operators are apprised via an alarm light panel.

Spectral responses that remain unmatched are passed to a subroutine designated Beat (Step 11). Similar to the characterization algorithm treatment, this logic interrogates data for beat frequency responses and applies appropriate limits. Should limits be exceeded, engine operators are informed.

If calculated  $K\text{-Factors}$ , for which there is no match in the baseline limit data, still exist, the data should be passed to the bearing subroutine (Step 12). The bearing subroutine calculates the theoretical  $K\text{-Factors}$  associated with all potential fault frequencies corresponding to the various bearings in the engine. For instance, the logic interrogates the unmatched  $K\text{-Factor}_{\text{calc}}$  to determine whether a specified alert or alarm limit has been exceeded for a particular sensor location. If so, a corresponding yellow or red alarm is initiated, and the data are dumped to permanent storage, thus calling to attention a potential problem.

The final step in the algorithm (Step 13) compares any random energy responses to specified amplitude limits. This process is completed in a subroutine designated Random. If no alarms are initiated, the data are sent to the circular file to be overwritten. Alternatively, an alarm is annunciated, and the data are sent to permanent storage.

## 5.6 OTHER CONSIDERATIONS

Obviously, the logic flow just described has been simplified significantly by not including transient digital parameters. For instance, a bearing thermocouple might prove invaluable in identifying a mechanical problem and would likely be incorporated into the logic.

Another example incorporates a scaling factor to increase/decrease established limits based on an operating condition which may be found to influence vibration characteristics for a particular operating condition (e.g., inlet temperature = 100 to 115°F) and sensor location.

Yet another obvious consideration is sensor location. For example, it would be unrealistic to apply No. 3 bearing fault frequencies to the No. 5 bearing health monitoring methodology. To circumvent needless number crunching and potential false alarms, engineering judgment must be applied in developing the logic and input files.

Importantly, the characterization and health monitoring methodologies discussed here may generally be extended to include vibration monitoring of case, gear box, and frame-mounted sensors. Planned operational capabilities of the HEMOS system incorporate additional algorithms to take advantage of these additional vibration sensors to more adequately determine relative health of test article hardware.

## **5.7 CADDMAS—A VEHICLE FOR HEMOS**

The Computer Assisted Dynamic Data Monitoring and Analysis System (CADDMAS) is an AEDC system which is being developed to acquire, store, process, and display dynamic signals from engines under evaluation in the AEDC Engine Test Facility (ETF). CADDMAS was first envisioned to tackle the huge task of processing strain-gage aeromechanical data and displaying results in near real-time. Huge volumes of data are currently generated at high sample rates (i.e., signal analysis to 32 KHz). CADDMAS uses a network of smart Integrated Sensors for preprocessing and a parallel architecture for additional processing and display to deliver engineering diagrams on-line and on demand from the user.

CADDMAS is designed to provide the computational horsepower to accomplish on-line visibility of analog parameters which drive test direction and ensure test article hardware health through component monitoring. A highly successful prototype CADDMAS was demonstrated in 1992 and is currently being used for test support in the ETF. The prototype system consists of dynamic data processing capabilities for 12 data channels sampled to provide analysis to 20 KHz. The system has been used to produce thousands of Campbell diagrams, spectral envelopes, and tracking plots in an on-line fashion with delivery to the end user in mere seconds. Similar off-line processing techniques may take up to two weeks to produce the same quality and quantity of information without the use of CADDMAS.

The AEDC Directorate of Technology—Propulsion Division (DOTP) end product CADDMAS will be capable of acquiring, processing, and displaying 48 channels to 50 KHz and an additional 24 channels to 20 KHz. The system will further be able to accept 32 transient digital data parameters at rates up to 1,000 sps.

CADDMAS is defining a new state-of-the-art for real-time dynamic data processing and analysis. With its astounding computational power, the system has many potential uses beyond on-line test monitoring of aeromechanical data. In fact, the current prototypical capabilities provide a stable vehicle on which to base the HEMOS system. Table 7 overviews the HEMOS system requirements and the corresponding CADDMAS capabilities (Ref. 6).

## **6.0 SUMMARY AND CONCLUSIONS**

### **6.1 SUMMARY**

To date, the goal of this research has been to develop an algorithm which can be applied to real-time monitoring of bearing vibration data from high-speed turbomachinery to alert engine operators of developing machine faults. Bearing fault diagnostic techniques have long been applied with great success to relatively low-speed, constant load machinery in the paper, power, and chemical industries. Application of these techniques to transiently operating turbine engines is in its relative infancy.

Two shortfalls determined through a literature survey concerning bearing vibrations were identified:

1. Most published work is devoted to a particular bearing application in a specific machine, and
2. Little work has been done to analyze the influence of bearing operating parameters on the vibratory environment.

This effort addresses these shortfalls by providing a means of adapting the real-time bearing health monitoring algorithm to any turbine engine family by incorporation of a user-defined input file, and developing a bearing health characterization algorithm which may be used to facilitate automated analysis of bearing vibration data. The health monitoring algorithm can be adjusted via the input file for each engine family specific application prior to testing. The characterization algorithm enables determination of applicable limits and influence of operating parameters in an offline mode.

This report strives to blend theoretical and practical considerations in developing algorithms that can be employed to characterize bearing health and to monitor incoming data for potential symptoms of developing hardware faults.

In Section 2.0, kinematic analysis is used to develop the bearing frequencies and related fault frequencies. These frequencies are often stated (and misstated) in the literature, but are seldom developed completely. The role of the fault frequencies in bearing fault detection is then discussed.

The physical quantities of vibration and the investigation of the interrelationships of displacement, velocity, and acceleration are defined and examined in Section 3.0. Examination of these mathematical relationships revealed the need for the health monitoring algorithm to be capable of incorporation of all three quantities into the logic. Frequency dependency and availability of proximity probes, velocity pick-ups, and accelerometers for turbine engine application necessitate this algorithm capability.

Additionally, Section 3.0 reviewed data presentation alternatives, primary bearing responses and the associated excitation sources, potential "health hazard" frequency responses, and limit application methodologies. The inherent advantages of using the amplitude versus K-Factor approach to limit application over the sliding mask approach were developed and discussed. Further, an overview of the bearing health monitoring algorithm and its inclusive *continuous* and *trend* modes of operation was introduced.

Analytical results from a single bearing housing mounted accelerometer were provided in Section 4.0. Data from accelerations and decelerations at 21 flight conditions were manually analyzed to develop trends of vibration amplitude with respect to various engine operating parameters. The enormity of this effort along with the realization that most turbine engine test articles are equipped with up to 12 vibration sensors and encompass 50 to 60 flight conditions illustrate the need for automating this analysis process. Preliminary programming of the characterization algorithm has been accomplished in FY93, and adaptation to the CADDMAS software will begin in FY94.

A culmination of research and analysis efforts was reached in Section 5.0 for development of bearing health criteria. The need for statistically categorizing engine family vibration characteristics was addressed, and a means of developing this statistical analysis was included as the bearing health characterization algorithm. Brief discussions of the role of operating environment on vibration characteristics and the significance of fault frequency combinations were then incorporated. A logic flow diagram for the actual real-time automated bearing health monitoring algorithm was presented and discussed. Finally, the role of CADDMAS capabilities versus HEMOS system requirements was introduced.

## 6.2 CONCLUSIONS

First, feasibility of developing an automated bearing health monitoring system through vibration analysis has been established. A literature survey revealed successes in the realm of monitoring for turbine engine faults through vibration investigation in both online and offline modes. Significant obstacles and lessons learned were also gleaned from the survey. Correct pre-teardown and post-mortem fault diagnoses, in which conditions leading to

catastrophic failure were identified minutes and even hours prior to the failure event, lent particular credence to system feasibility.

Second, the relationships of peak-to-peak displacement, peak velocity, and peak acceleration indicate a significant influence of frequency of vibration on the measured amplitudes. Displacement, for example, is an excellent measure of vibration at lower frequencies, but becomes practically useless at frequencies above 1000 Hz. Hence, each measurement quantity of vibration has a range of frequencies over which satisfactory amplitude resolution is maintained. Experience in turbine engine bearing vibration data analysis suggests the following frequency ranges:

displacement – 0 to 500 Hz,

velocity – 200 to 1200 Hz, and

acceleration – 800 to 10,000 Hz.

Importantly, most engine-mounted accelerometers provide a flat frequency response from 0 to 10,000 Hz. This means that amplitude outputs are reliable over this range. At lower frequencies, however, note that units of displacement or velocity give a more intuitive feel for the vibration amplitude. The algorithms require special attention to the vibration sensors installed and the inherent advantages and disadvantages when specifying applicable alert and alarm limits.

Third, the K-Factor approach to limit application is a key development. Using this methodology, statistical analyses can be conducted which will provide meaningful amplitude alert and alarm limits as a function of constant K-Factor<sub>i</sub>. This eliminates the huge development task associated with programming alert and alarm limits, which are functions of the frequencies of vibration (i.e., the sliding mask).

Fourth, analysis of a single bearing-mounted accelerometer responses to accelerations and decelerations at a variety of flight conditions yielded significant results. Though trending studies of the influence of several operating parameters were accomplished, the primary excitation source was always rotor unbalance (i.e., the highest amplitudes of vibration were always measured at the highest rotor speeds, regardless of operating environment). If proven using the bearing health characterization algorithm, this postulation may greatly simplify the real-time health monitoring methodology.

Fifth, two algorithms were developed. The first, bearing health characterization algorithm, should allow automated analysis to statistically band common responses for a given engine



component (e.g., bearing) across a wide array of operating conditions and speeds. From this analysis, it is judged that meaningful alert and alarm limits can be specified for individual engine families and sensor placement locations. The second algorithm, real-time bearing health monitoring algorithm, can be further developed to provide a means of real-time avoidance of catastrophic failures by alerting engine operators to potential developing hardware faults. Future HEMOS plans include algorithm expansion to encompass all engine-mounted vibration sensors (i.e., case, gear box, etc.) and incorporate transient digital signals to enhance overall engine health determination.

Finally, the efforts presented in this report establish the methodologies by which meaningful characterization of relative bearing health may be achieved. The algorithms must next be automated and refined, and in-depth analyses must be conducted for a variety of engine families. The ultimate goal of saving turbine engines from total self destruction appears to be within reach. The algorithms developed in this report should provide a means of reaching that goal.

## REFERENCES

1. Braun, S. *Mechanical Signature Analysis: Theory and Applications*. London: Academic Press, 1986.
2. Blake, Michael P. and William S. Mitchell. *Vibration and Acoustic Measurement Handbook*. New York—Washington: Spartan Books, 1972.
3. Smith, Richard L. "Rolling Element Bearing Diagnostics with Lasers, Microphones, and Accelerometers." 46th Meeting of the Mechanical Failures Prevention Group, Va. Beach, VA, April 7-9, 1992.
4. Pettigrew, James L. "Diagnostics Look at Engine Condition." 44th Meeting of the Mechanical Failures Prevention Group, Virginia Beach, VA, April 3-5, 1990.
5. Carr, H. R. "UK Military Engine Vibration Monitoring Experience." SAE E-32 Engine Health Monitoring Committee Symposium—Vibration Monitoring and Analysis, Zurich, Switzerland, October 23-24, 1990.
6. Hite, S. W. "Real Time Vibration Health Monitoring For Transiently Operating High-Speed Turbomachinery." 47th Meeting of the Mechanical Failures Prevention Group, Virginia Beach, VA, April 13-16, 1993.

7. Li, C. J. and J. Ma. "Bearing Localized Defect Detection Through Wavelet Decomposition of Vibrations." 46th Meeting of the Mechanical Failures Prevention Group, Virginia Beach, VA, April 7-9, 1992.
8. Harris, T. A. *Rolling Bearing Analysis*. Second Edition. New York: John Wiley and Sons, 1984.
9. White, R. F. "Vibratory Velocity; A Measure of the Destructive Potential of Vibration." Allison Laboratory Report, A-9628, August 1970.
10. Collatz, Lothar. *Functional Analysis and Numerical Mathematics*. New York—London: Academic Press, 1966.
11. Jackson, C. J. *The Practical Vibration Primer*. Second Printing. Houston: Gulf Publishing Company, 1981.

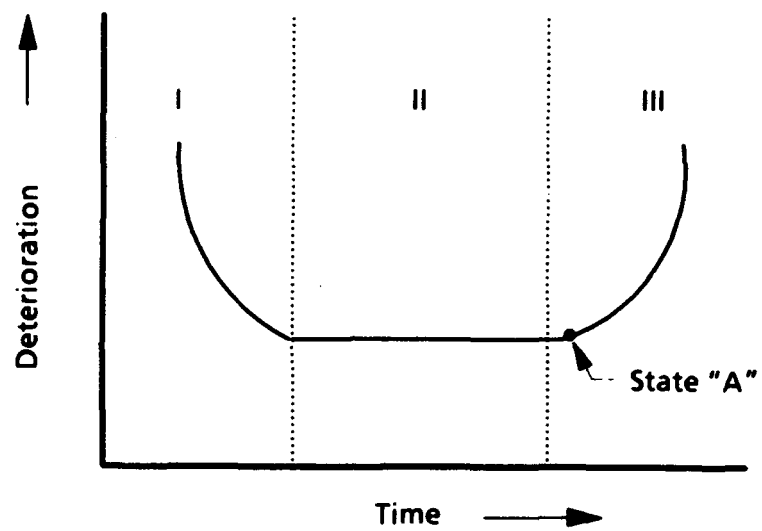


**Figure 1. Phases of machine deterioration.**

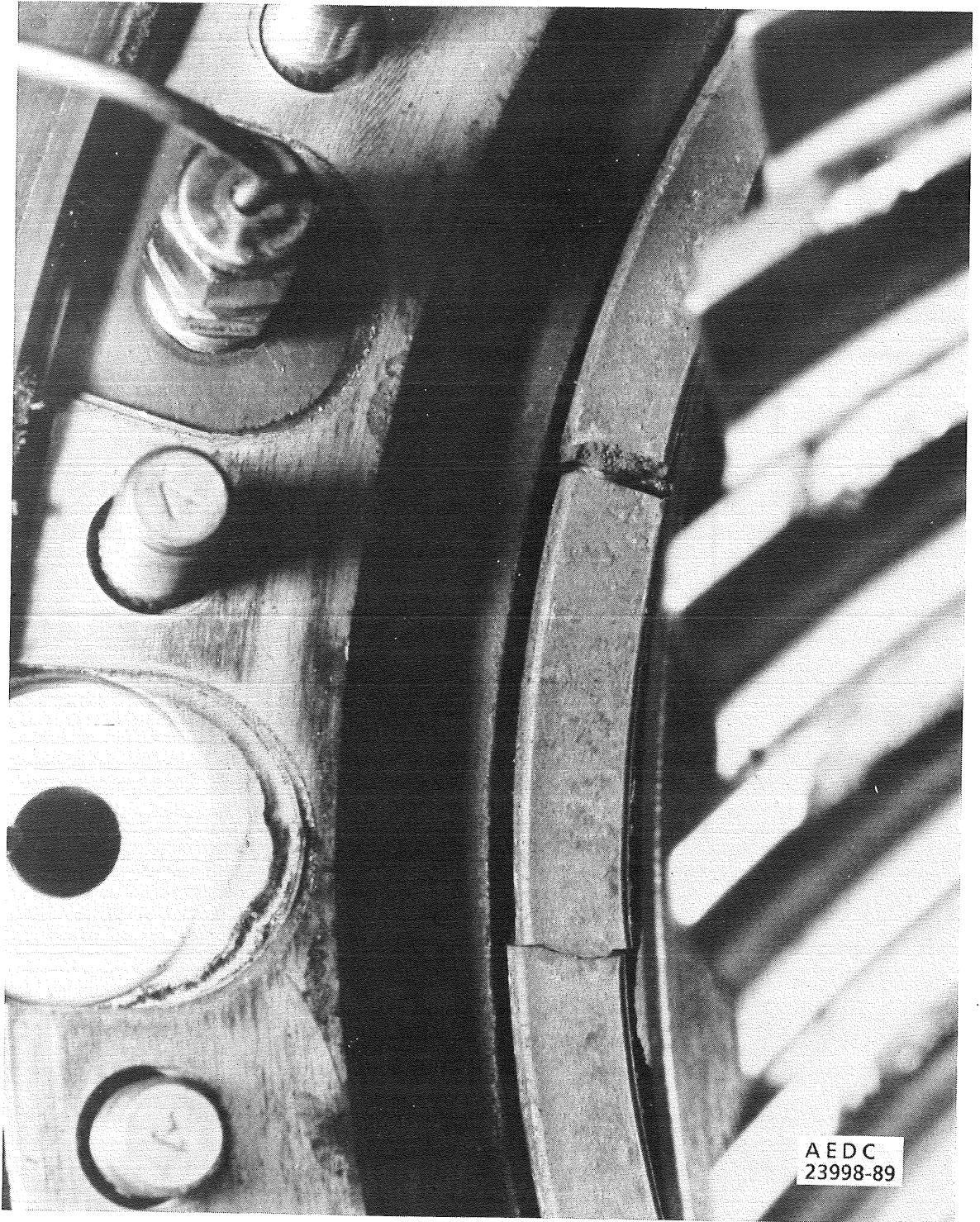


**Figure 2. Failed ball element thrust bearing.**

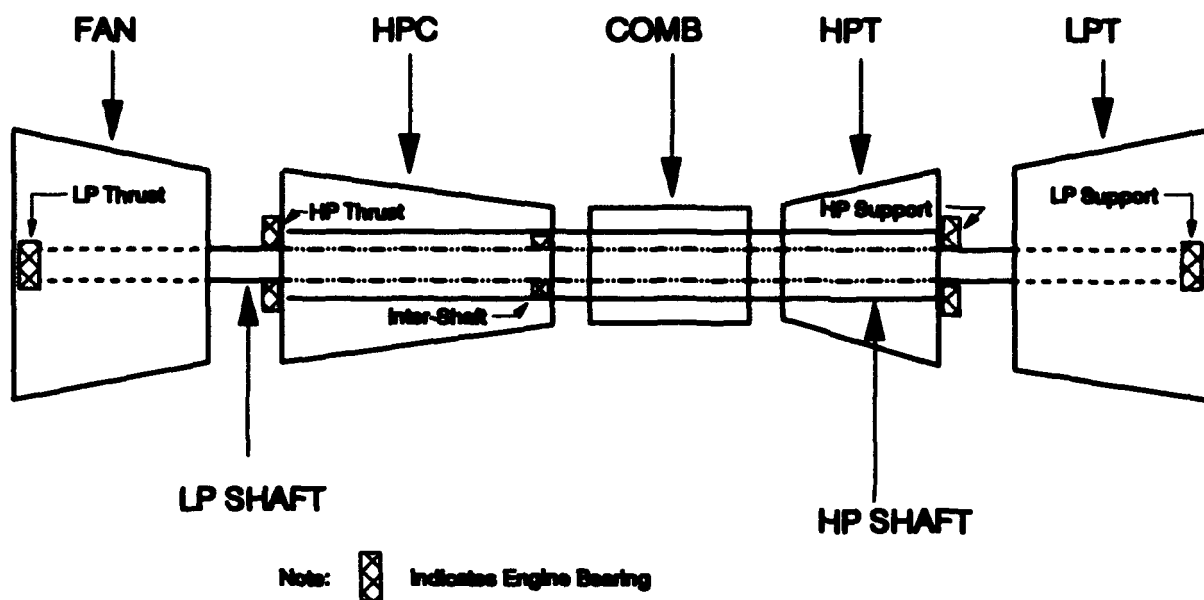


Figure 3. Simplified schematic of a turbofan engine.

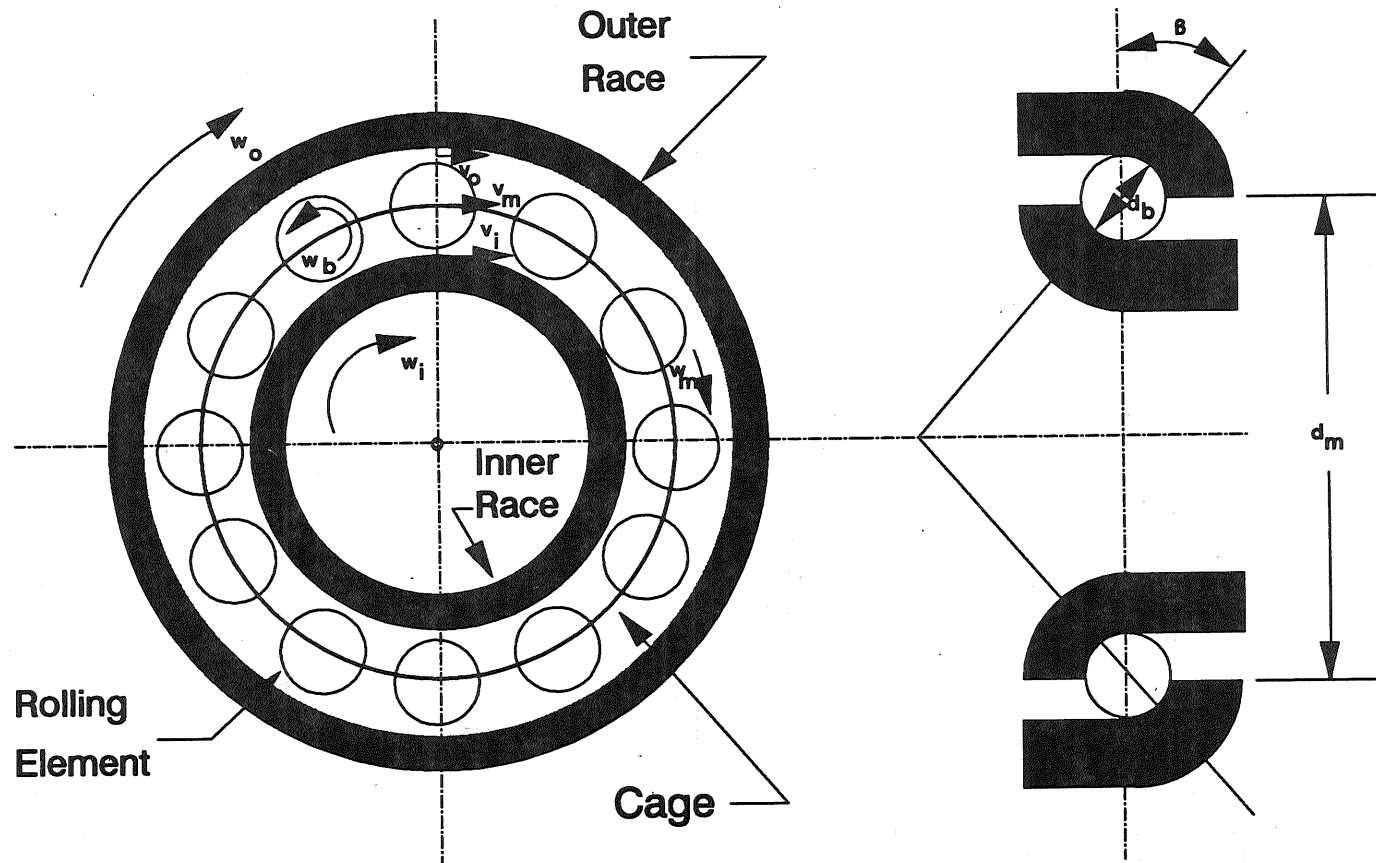
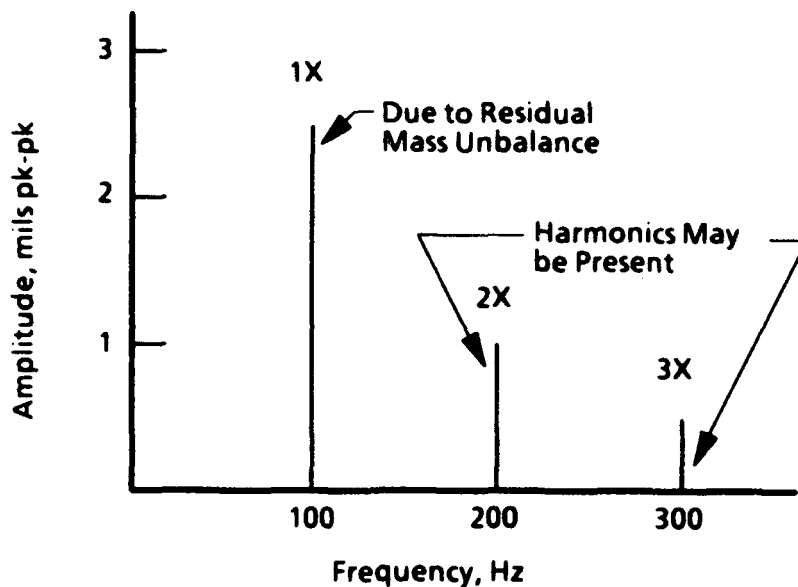
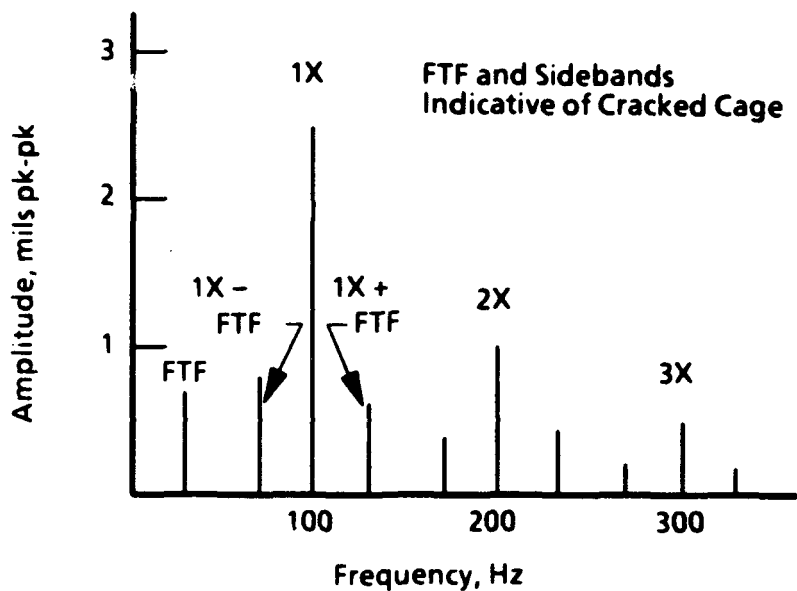


Figure 4. Rolling element bearing geometry and motion.



**Figure 5. Typical "healthy" bearing spectrum.**



**Figure 6. Deteriorated bearing spectrum.**

P = 0.09 ips pk  
= 4 mils pk-pk  
= 0.01 g's pk

Q = 0.065 ips pk  
= 0.002 mils pk-pk  
= 10 g's pk

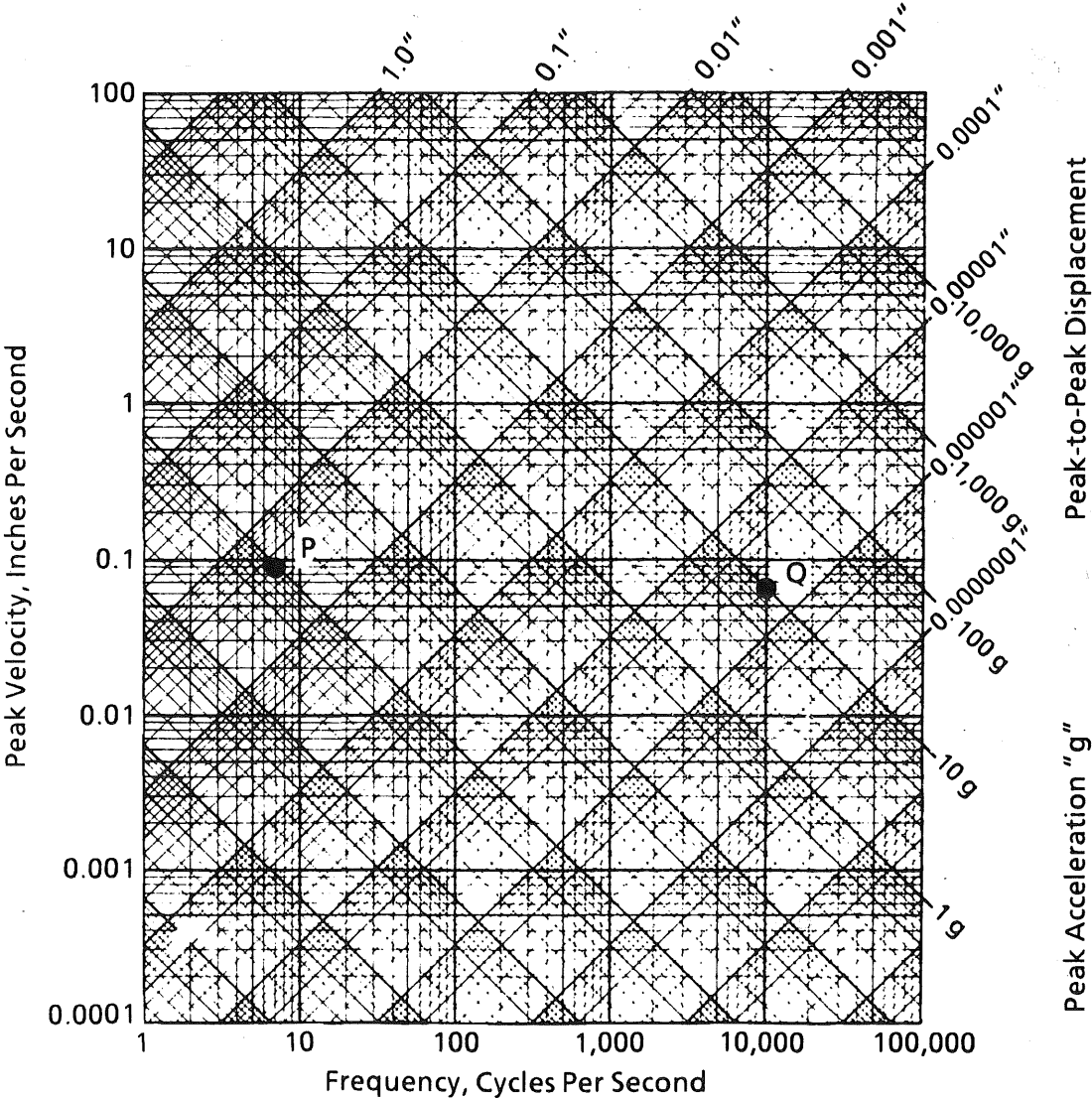
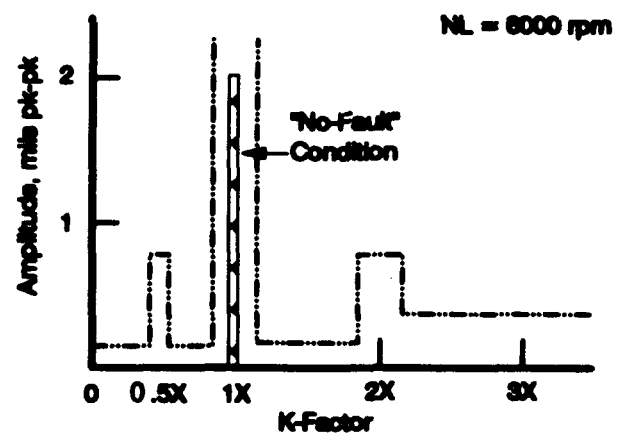
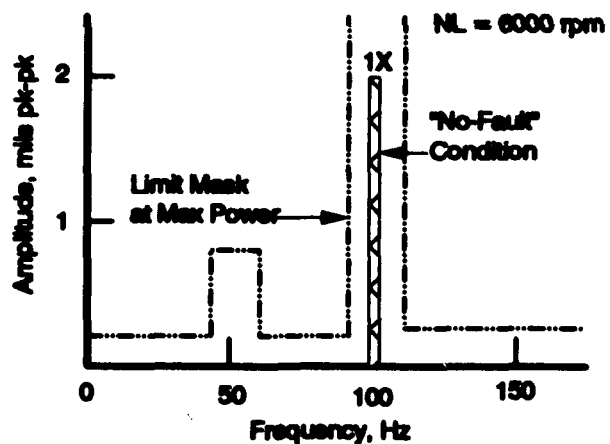
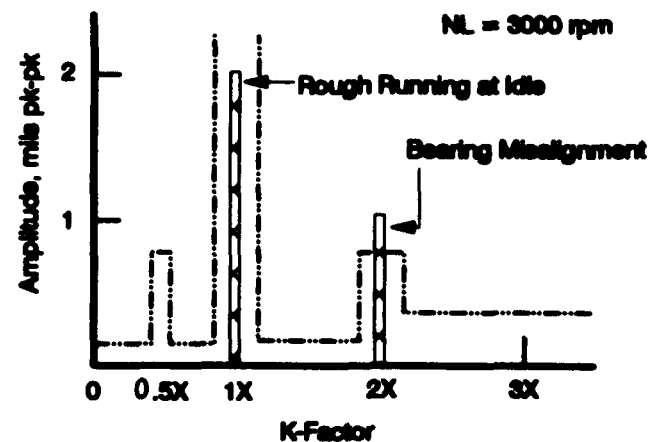
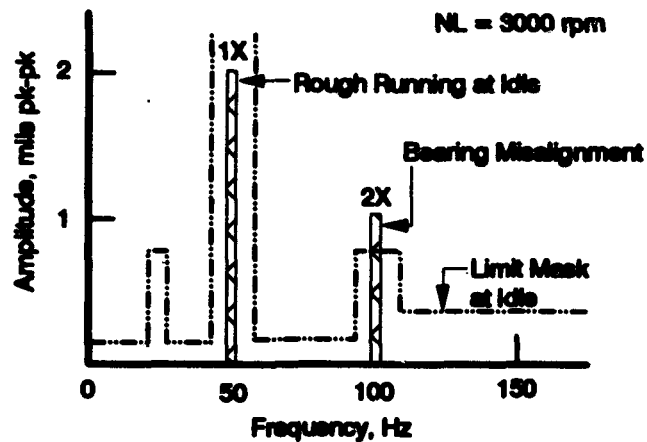


Figure 7. Vibration unit conversion nomograph (Ref. 11).





a. Sliding mask limit application methodology (note change in mask with speed from top to bottom)

b. K-Factor limit application methodology (no change in mask with speed)

Figure 8. Limit application methodologies.

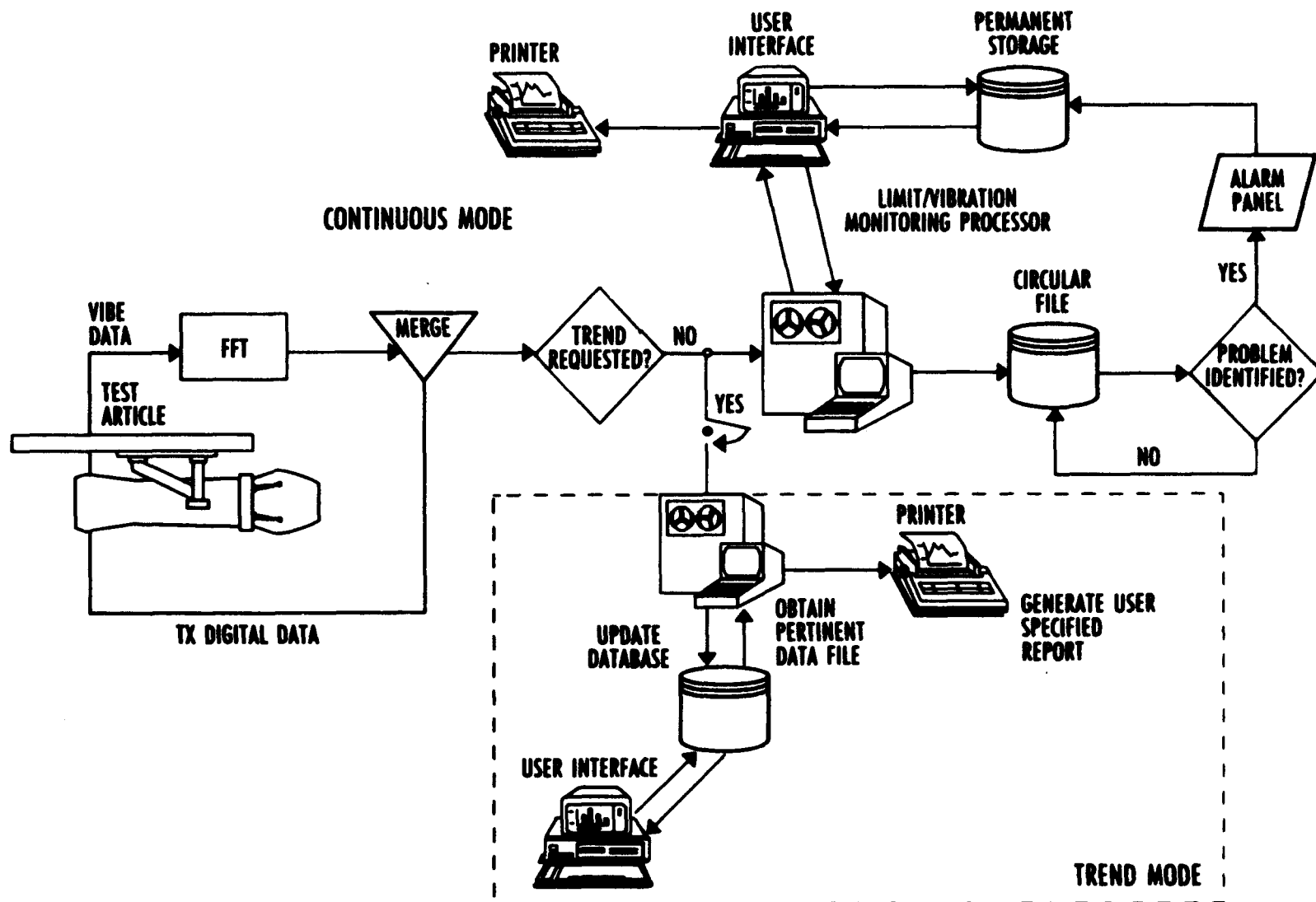
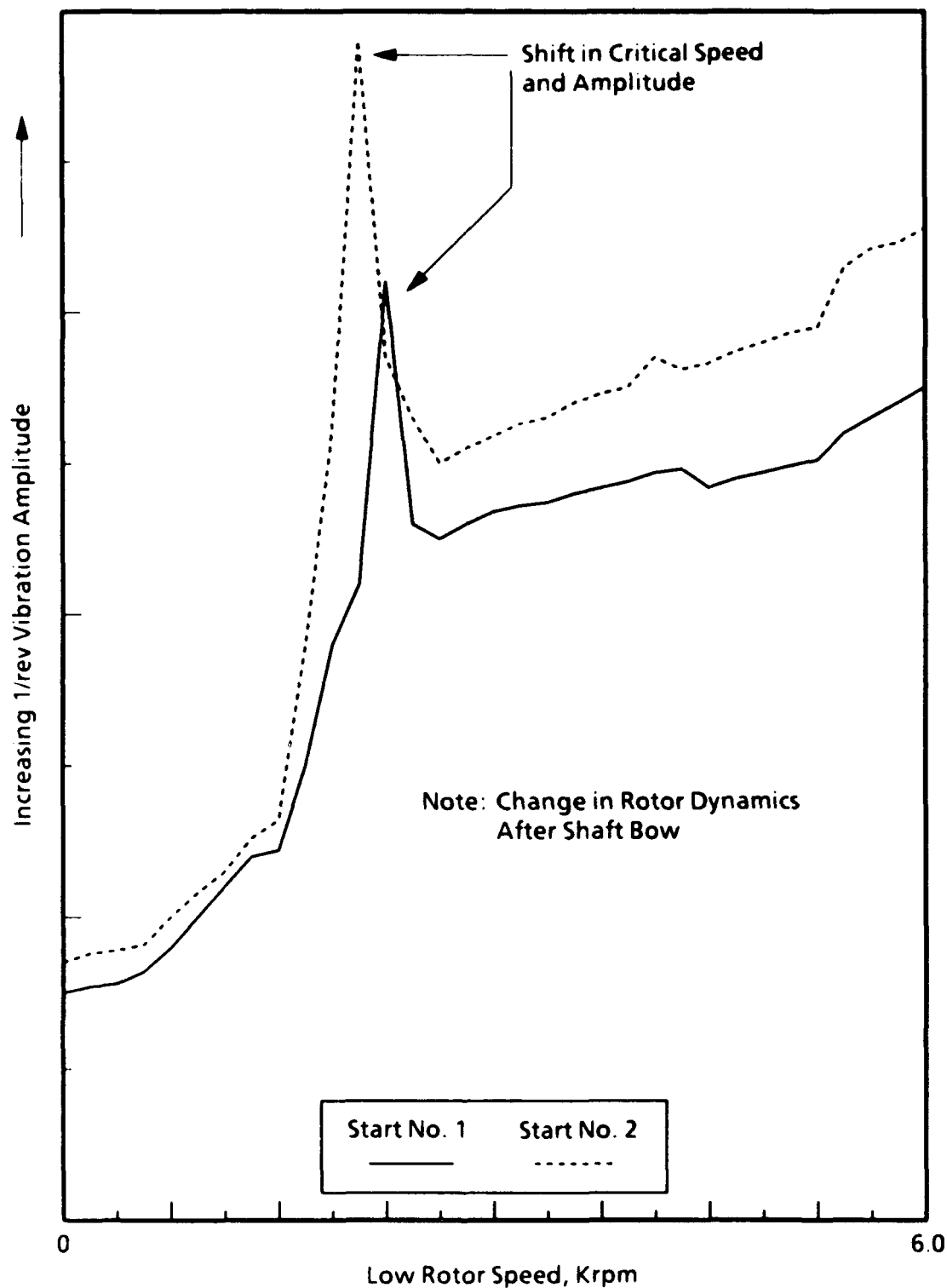


Figure 9. Overview of hardware and data flow.



**Figure 10. Tracking plot of 1/rev vibration for consecutive engine starts.**

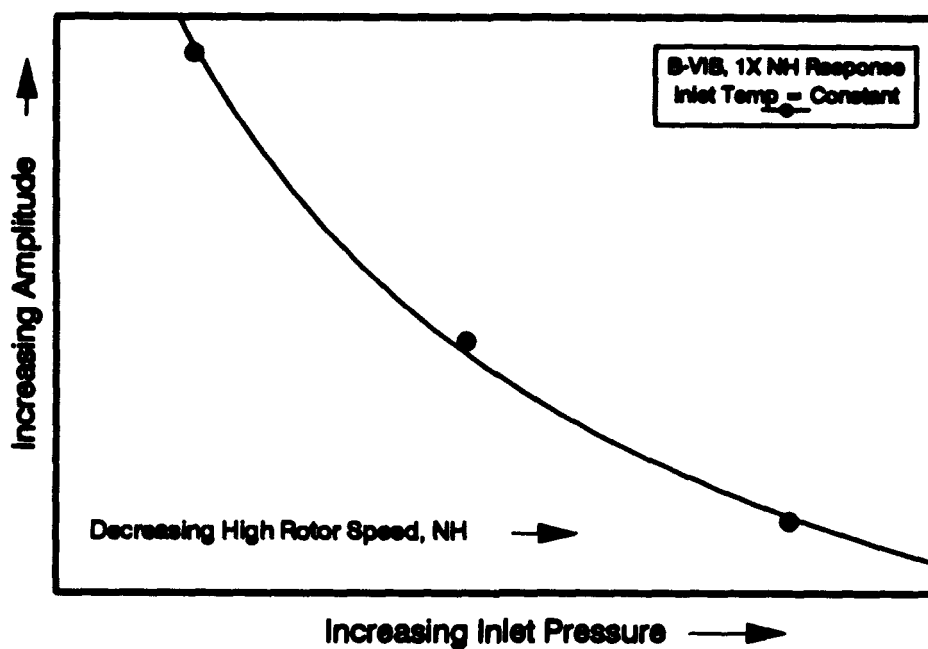


Figure 11. Vibration amplitude as a function of inlet pressure.

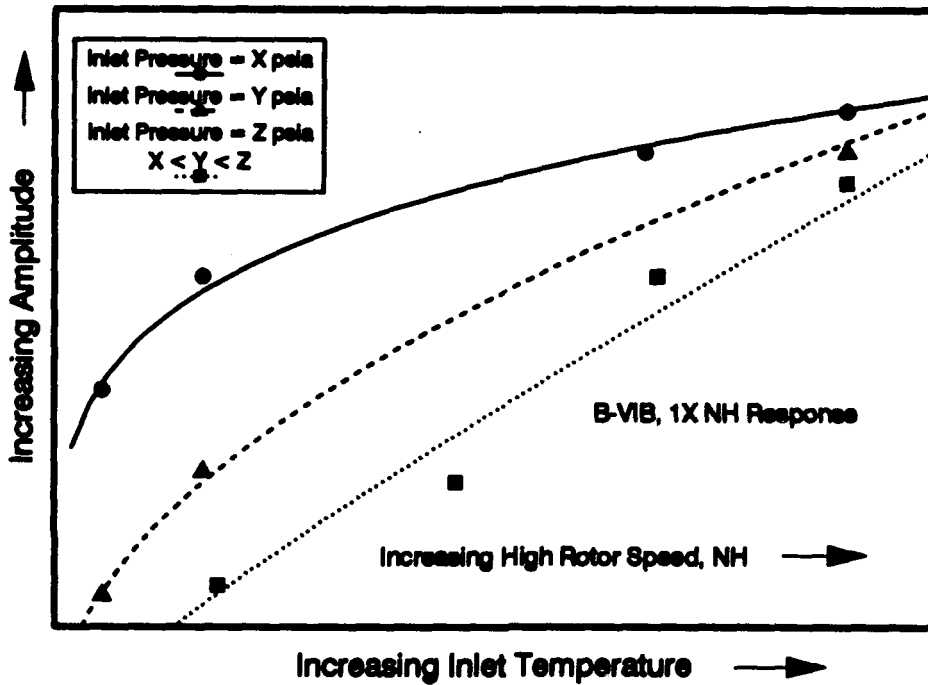


Figure 12. Vibration amplitude as a function of inlet temperature.

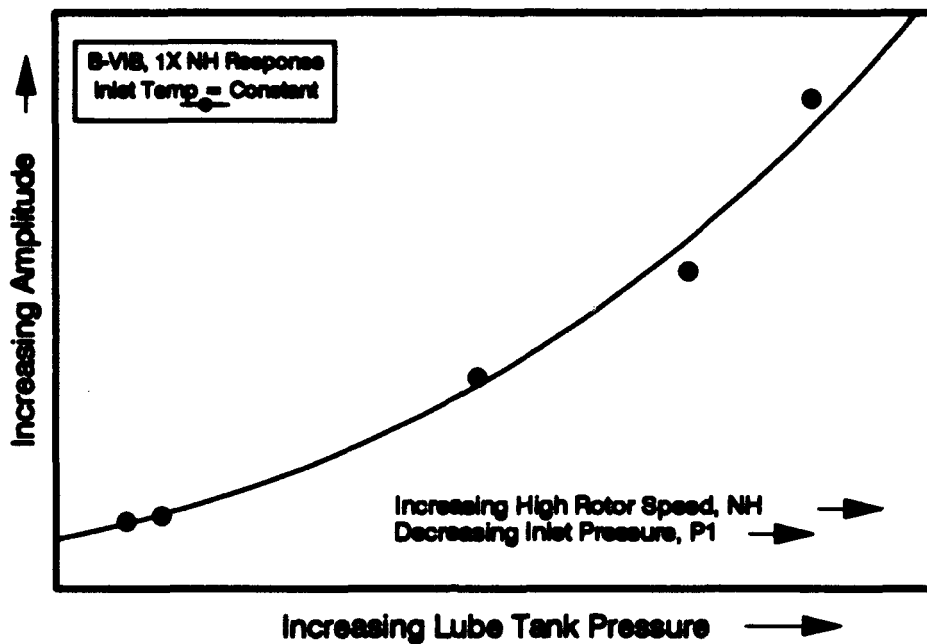


Figure 13. Vibration amplitude as a function of lube tank pressure.

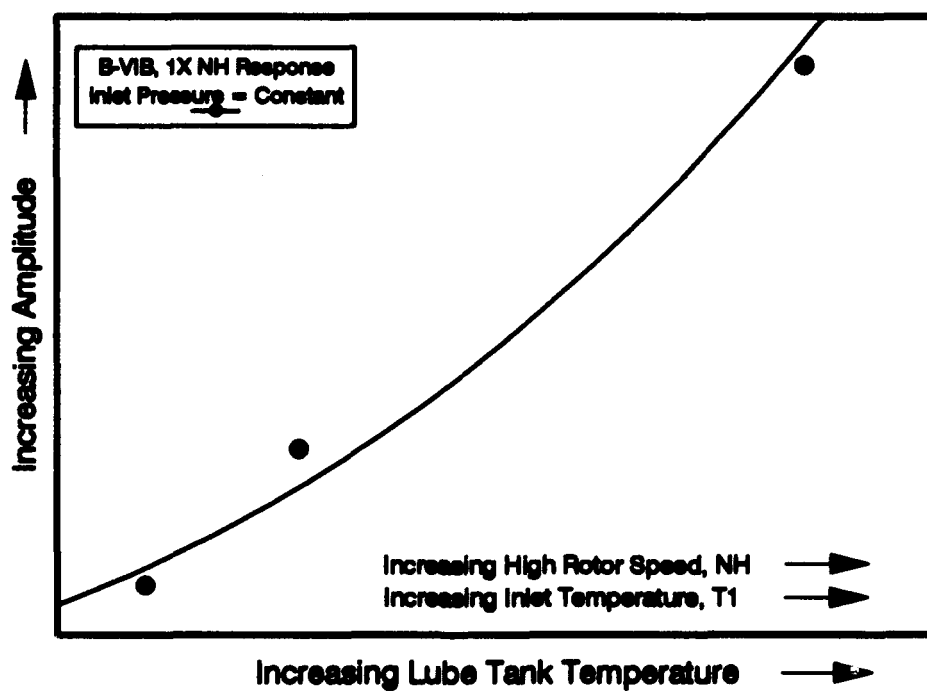


Figure 14. Vibration amplitude as a function of lube tank temperature.

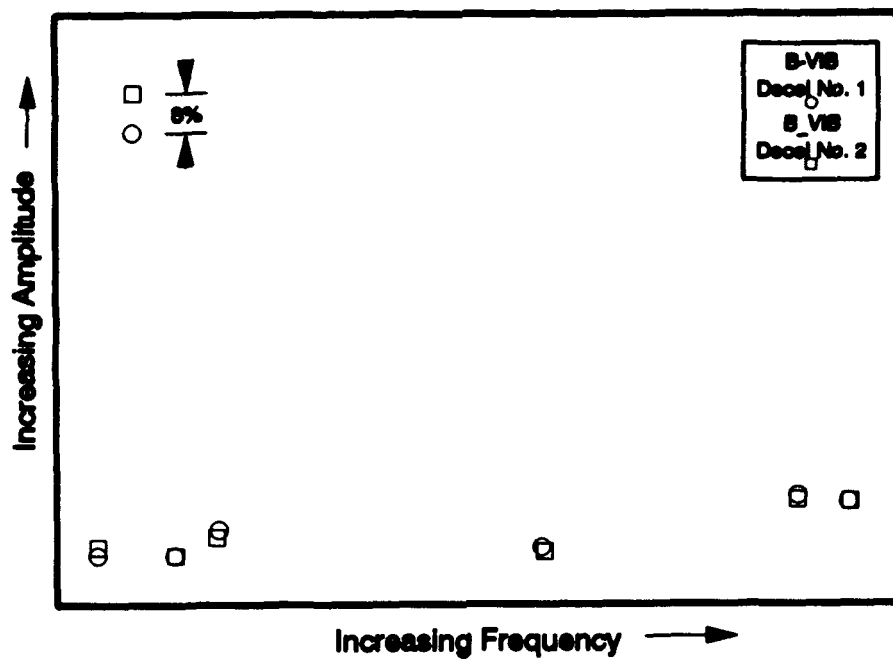


Figure 15. Response amplitude repeatability — consecutive decelerations.

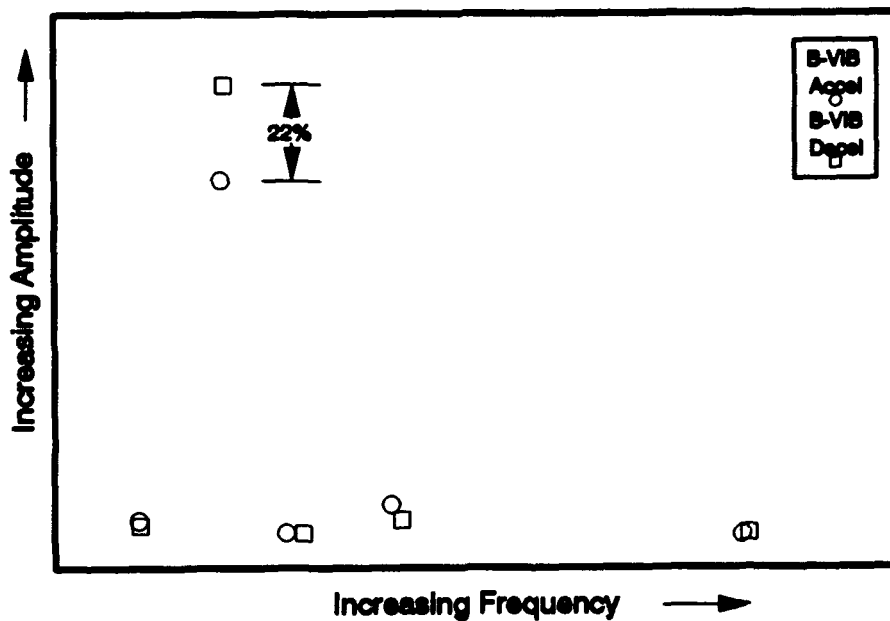


Figure 16. Response amplitude repeatability — acceleration to deceleration variation at constant inlet conditions.



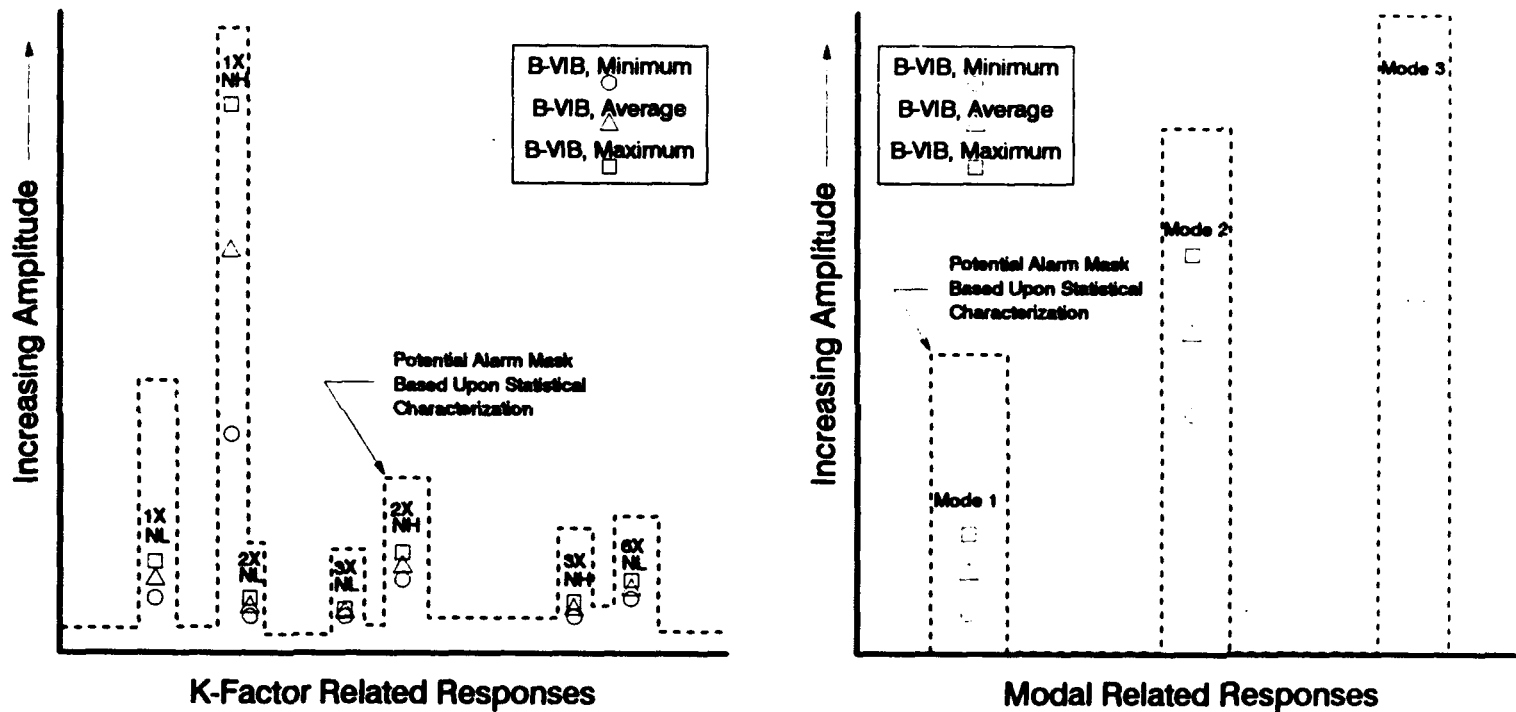


Figure 18. Sample plots of amplitude versus K-Factor and amplitude versus mode.



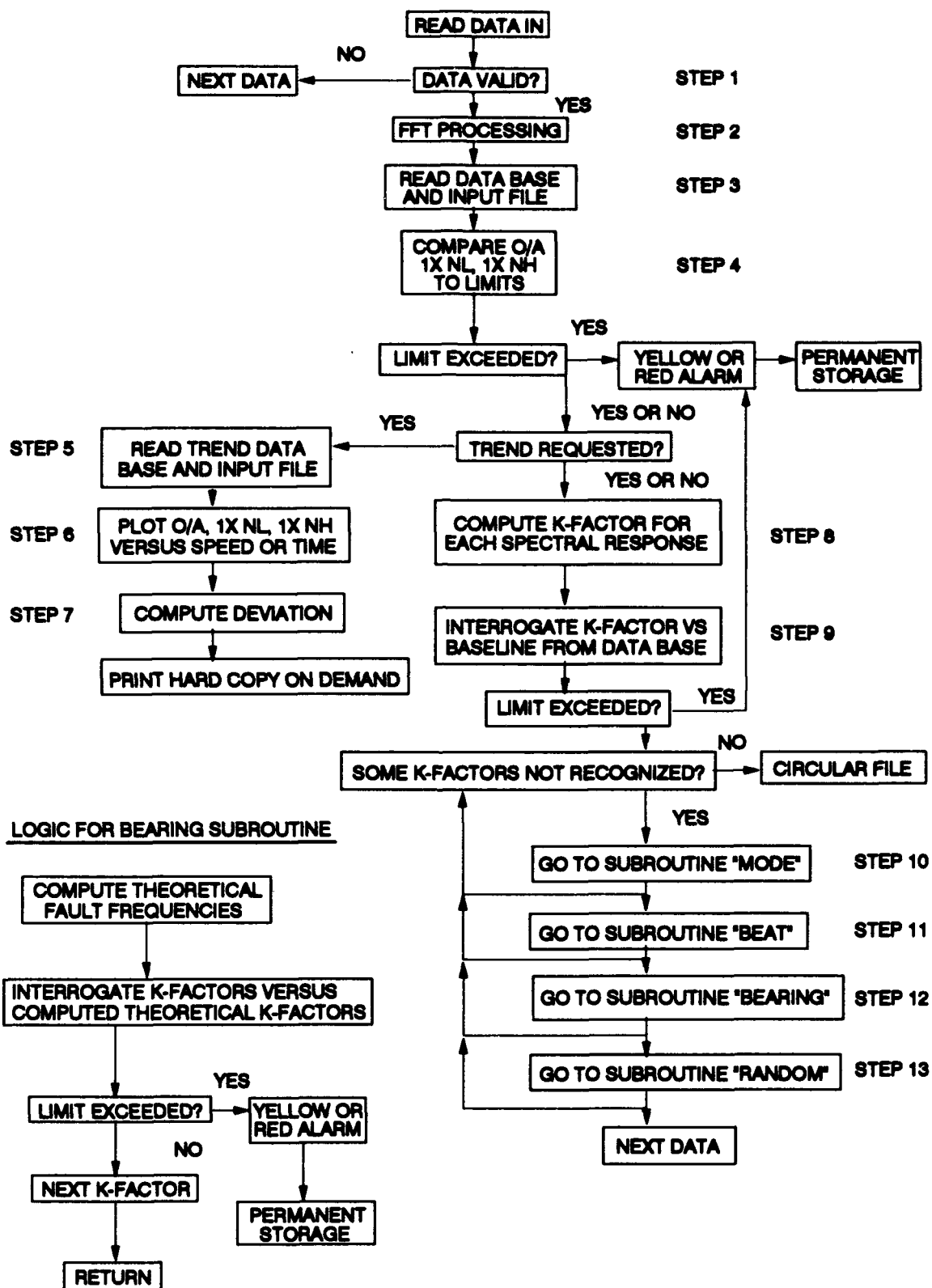


Figure 19. Real-time bearing health monitoring algorithm flow chart.

**Table 1. Rolling Element Bearing Defect Frequencies**

Component	Frequency	Significance
Rolling element train defect (FTF)	$\frac{1}{2}f_i(1 - \mu)$	Caused by an irregularity of a rolling element on the cage
Rolling element defect (BSF)	$\frac{1}{2}m(d_m/d_b)f_i(1 - \mu^2)$	Irregularities alternately strike inner and outer races
Outer race defect (BPFO)	$(n/2)f_i(1 - \mu)$	Irregularity on race generates impacting with each rolling element pass
Inner race defect (BPFI)	$(n/2)f_i(1 + \mu)$	Irregularity on race generates impacting with each rolling element pass

Where

- $f_i$  = inner race frequency,  $N/60$ , in Hz
- $N$  = rotational speed in rpm
- $m$  = number of rolling element irregularities
- $d_m$  = mean bearing diameter (cf. Fig. 3)
- $d_b$  = rolling element diameter (cf. Fig. 3)
- $n$  = number of rolling elements
- $\mu = (d_b/d_m) \cos \beta$
- $\beta$  = bearing contact angle (cf. Fig. 3)

**Table 2. Characterization Algorithm Input File**

Valid Input(s) Title Card 2	Explanation of inputs Test program identifier
10 mils pk-pk 2 1 No. 3 Bearing 1, 2, 11, 12	100-percent amplitude scale Integer number of components Component number and name Dynamic numbers assigned to dynamic channels for this component
0.2 mils pk-pk	Threshold amplitude and units to be applied for this component
2	Speed switch, NSW, for component 1 = low rotor, 2 = high rotor
2 1 Housing Resonance 3000, 780, 790 9000, 760, 770	Number of defined modal responses Mode number and name Min speed, min freq, max freq Max speed, min freq, max freq
2 Frame Strut Resonance 3000, 1550, 1590 9000, 1520, 1560	Repeat for second mode
2 1 Cable Whip 3000, 0, 15 9000, 0, 15	Number of defined noise bands Noise band number and name Min speed, min freq, max freq Max speed, min freq, max freq
2 TVA 3000, 59, 61 9000, 59, 61	Repeat for second noise band
2 No. 5 Bearing	Repeat blocks above for all components beginning with component number and name

**Table 3. Sample Statistical Output File**

Output Data	Significance
<b>1 B-VIB</b> 0.2 <b>1X NH</b> 389, 0.3, 2.8, 1.4, 0.67	Parameter number and name Threshold applied to data Component of vibration No. of matched responses, min, max, avg, and deviation
<b>2X NH</b> 121, 0.4, 1.1, 0.8, 0.32  <b>1X NL</b> 212, 0.6, 1.4, 0.8, 0.41	Repeat for all engine order related responses
<b>2X NL</b> 34, 0.3, 0.4, 0.4, 0.05	
<b>1 Housing Resonance</b> 166, 0.3, 0.5, 0.4, 0.10	Mode number and name No. of matched responses, min, max, avg, and deviation
<b>1 Beat: (NH – NL)/60</b> 59, 0.3, 0.7, 0.5, 0.20	Beat freq number and name No. of matched responses, min, max, avg, and deviation
<b>Random</b> 11, 0.3, 0.4, 0.4, 0.05	Random response indicator No. of random responses, min, max, avg, and deviation
<b>2 C-VIB</b>	Next parameter number and name Repeat above beginning with threshold

**Table 4. Sample Histogram**

Amplitude Range, percent	No. of Matches
0 – 20	1185
21 – 40	770
41 – 60	212
61 – 80	11
81 – 100	2

**Table 5. Fault Frequency Combinations and Diagnoses**

Defect or Condition	Frequency	Spectrum Shape	Diagnosis
Inner race defect	BPFI and mult	Decreasing amplitude harmonics	Shallow flaking
Inner race defects	BPFI and mult	Decreasing amplitude harmonics and modulation at running speed	Failure imminent; shutdown required
Outer race defects	BPFO and mult	Decreasing amplitude harmonics	Shallow flaking
Cage and outer race defects	BPFO and mult and FTF	FTF modulation at higher frequencies	Failure imminent; shutdown required
Cage, balls, and outer race defects	BPFO and mult and FTF	BPFO modulated by FTF	Cage or roller defects
Outer race defects	BPFO and mult	Increasing amplitude harmonics	Deep fatigue spall
Defects on inner and outer races	BPFO and BPFI	Bearing frequencies and sum and difference frequencies	Worsening defects
Inner race and ball defect	BPFI and BSF	Decreasing amplitude harmonics and BPFI modulated by BSF	Worsening defects
Cage defect	FTF and mult	Steady amplitude harmonics of FTF	Badly worn or cracked cage

Note: Adapted from: Eshleman, R. L. "Rolling Element Bearing Analysis." Vibration Institute: Machinery Vibration Analysis I, Course Notes, Nashville, Tn. November 17-20, 1987.

**Table 6. Health Monitoring Algorithm Input File**

Valid Input(s)	Explanation of Inputs
Title Card 1 Title Card 2	Engine identifier Test program identifier
10 mils pk-pk 1 1 No. 3 Bearing 1, 2, 11, 12	100-percent amplitude scale Integer number of components Component number and name Dynamic numbers assigned to dynamic channels for this component
12, 6.4, 0.5, 8	Component geometry: No. rolling elements, $d_m$ , $d_b$ , $\beta$
0.2 mils pk-pk	Threshold amplitude and units to be applied for this component
2	Speed switch, NSW, for component 1 = low rotor, 2 = high rotor
Curve 1	Name of file where manufacturer's specified O/A, 1X NH, 1X NL limits are stored
1 30K/0.9 Acceleration Curve 2, 1.5	Number/names of trend windows Baseline trend info file and allowable standard deviation
Curve 3	Filename where NH related K-Factor alert and alarm limits are stored
Curve 4	Filename where NL related K-Factor alert and alarm limits are stored

**Table 6. Concluded**

Valid Input(s)	Explanation of Inputs
1	Number of defined modal responses
1 Housing Resonance	Mode number and name
3000, 780, 790	Min speed, min freq, max freq
9000, 760, 770	Max speed, min freq, max freq
1.0, 1.5 mils pk-pk	Specified alert and alarm limits
1 Beat: (NH – NL)/60	Numbers and names of defined beat frequencies
0.6, 0.8 mils pk-pk	Specified alert and alarm limits
FTF, 0.4, 0.8 BSF, 0.4, 0.8 BPFO, 0.4, 0.8 BPFI, 0.4, 0.8	Bearing fault frequency specified alert and alarm limits
0.6, 1.2 mils pk-pk	Specified alert and alarm limits for random vibration
1	Number of defined noise bands
1 Cable Whip	Noise band number and name
3000, 0, 15	Min speed, min freq, max freq
9000, 0, 15	Max speed, min freq, max freq

**Table 7. CADDMAS Capabilities Versus HEMOS Requirements (Ref. 6)**

	CADDMAS Capabilities	HEMOS Requirements
Data Validity Check	Frequency versus RMS	Required
No. Input Channels	48 Dynamic	12 Dynamic
	40 Digital	20 Digital
Physical Quantities	Acc Vel Dis	Acc Vel Dis
Frequency Range	0-50 kHz	0-8 kHz
Frequency Resolution	$\pm 25$ Hz @ 10 kHz	$\pm 5$ Hz
Amplitude Resolution	$\pm 2$ percent	$\pm 5$ percent
Data Storage	70 + GB	38.9 GB
Limit Application	TBD	K-Factor Approach
Plot Alternatives	TBD	Many

TBD Indicates: To Be Developed



## NOMENCLATURE

<u>Symbol</u>	<u>Description</u>
A	Amplitude of vibration
a	Acceleration
Acc	Acceleration
AEDC	Arnold Engineering Development Center
B	Peak displacement
BEAT $f$	Beat frequency
B-VIB	Bearing housing mounted accelerometer
BPFI	Ball passing frequency—inner race
BPFO	Ball passing frequency—outer race
BSF	Ball spin frequency (also $f_b$ )
$\beta$	Bearing contact angle
CADDMAS	Computer Assisted Dynamic Data Monitoring and Analysis System
COMB	Combustion chamber
cps	Cycles per second (also Hz)
CRT	Cathode ray tube
D	Time-dependent displacement of a body
d	Peak-to-peak displacement
$d_b$	Rolling element diameter
$d_i$	Inner race diameter
Disp	Displacement
$d_m$	Bearing mean (or pitch) diameter
DN	Bearing diameter times running speed
$d_o$	Outer race diameter
DOTP	Directorate of Technology—Propulsion Division
ETF	Engine Test Facility
FFT	Fast Fourier Transform
FTF	Fundamental train frequency (also $f_m$ )
freq	Frequency (also $f$ )
$f$	Frequency (also freq)

<u>Symbol</u>	<u>Description</u>
$f_b$	Rolling element frequency
$f_{\text{fixed}}$	Inner race frequency relative to fixed reference frame
$f_i$	Inner race frequency
$f_m$	Rolling element train frequency (also FTF)
$f_{\text{mode}}$	Modal frequency
$f_{\text{noise}}$	Noise frequency
$f_o$	Outer race frequency
$g$	Unit of acceleration, 386.087 in./sec <sup>2</sup>
HEMOS	Health Monitoring System
HP	High pressure
HPC	High-pressure compressor
HPT	High-pressure turbine
Hz	Hertz (also cps)
in./sec	Inches per second (also ips)
in./sec <sup>2</sup>	Inches per second per second
K	K-Factor
K-Factor <sub>calc</sub>	Calculated K-Factor
Kft	Kilofeet
LP	Low pressure
LPT	Low-pressure turbine
m	Number of rolling element irregularities
max	Maximum
mil	0.001 in.
min	Minimum
mult	Multiples
$\mu$	$(d_b/d_m)$ cosine $\beta$
N	Shaft running speed
n	Number of bearing rolling elements
NH	High rotor speed
NL	Low rotor speed
NSW	Rotor speed switch

<u>Symbol</u>	<u>Description</u>
O/A	Overall vibration
pk	Peak
pk-pk	Peak to peak
PTO	Power take-off
r	Distance from axis of rotation
$r_i$	Distance from shaft center to point on surface of inner race
$r_{mi}$	Distance from rolling element center to point of contact with inner race
rms	Root-mean-square
$r_o$	Distance from shaft center to point on surface of outer race
sps	Samples per second
STD DEV	Standard deviation
TVA	Tennessee Valley Authority
v	Velocity
$v_b$	Rolling element velocity
Vel	Velocity
$v_i$	Inner race velocity
$v_m$	Rolling element train velocity
$v_o$	Outer race velocity
$V_{pk-pk}$	Peak-to-peak voltage
w	Angular velocity
$w_b$	Rolling element angular velocity
$w_{fixed}$	Inner race angular velocity relative to fixed reference frame
$w_i$	Inner race angular velocity
$w_m$	Rolling element train angular velocity
$w_{mi}$	Rolling element train angular velocity relative to the inner race
$w_o$	Outer race angular velocity
1/rev	Once per revolution
1X, 2X, 3X,	Multiples of running speed